PNNL-16639

Pacific Northwest
National Laboratory
Operated by Battelle for the
U.S. Department of Energy

Summary of Chalcogenide Glass Processing: Wet-Etching and Photolithography

B. J. Riley
S. K. Sundaram
B. R. Johnson
L. Saraf

December 2006

Work performed for Battelle Memorial Institute/DARPA

Prepared for the U.S. Department of Energy
under Contract DE-AC05-76RL01830

DISCLAIMER

PACIFIC NORTHWEST NATIONAL LABORATORY
operated by
BATTELLE
for the
UNITED STATES DEPARTMENT OF ENERGY
under Contract DE-ACO5-76RL01830

Printed in the United States of America

Available to DOE and DOE contractors from the
Office of Scientific and Technical Information,
P.O. Box 62, Oak Ridge, TN 37831-0062;
ph: (865) 576-8401
fax: (865) 576 5728
email: reports@adonis.osti.gov

Available to the public from the National Technical Information Service,
U.S. Department of Commerce, 5285 Port Royal Rd., Springfield, VA 22161
ph: (800) 553-6847
fax: (703) 605-6900
email: orders@nits.fedworld.gov
online ordering: http://www.ntis.gov/ordering.htm

PNNL-16639

Summary of Chalcogenide Glass Processing: Wet-Etching and Photolithography

B. J. Riley
S. K. Sundaram
B. R. Johnson
L. Saraf

December 2006

Work performed for Battelle Memorial Institute/DARPA

Prepared for the U.S. Department of Energy
under Contract DE-AC05-76RL01830

Pacific Northwest National Laboratory
Richland, Washington 99354

Summary

Our main goals were to obtain a single variable etch rate curve of etch depth per time versus NaOH overall solution concentration in molarity (M) and to see the difference in etch rate between a given etchant when used on the different chalcogenide stoichiometries. Chalcogenide glasses are made by combining chalcogen elements S, Se, and Te with Group IV and/or V elements. The etch rate curves can be used in selecting etching conditions for specific stoichiometry and film thickness. This report describes a study designed to explore the etchability of two different chalcogenide materials, As_2S_3 and $As_{24}S_{38}Se_{38}$, when subjected to photolithographic wet-etching techniques for potential application in fabrication of photonic bandgap (PBG) structures that will function in the long-wave infrared (LWIR) regime.

We chose arbitrarily a 4 M concentration of sodium hydroxide (NaOH) chosen for the experiments reported. When making the etchants for this study, the concentration of 4 M NaOH was altered while keeping the volume ratios of isopropyl alcohol (IPA) and deionized water (DIW) (1:2, respectively). All the variables in the etching process as well as the challenges involved in the etching study are elucidated in this report. The stock etchant, 1:25:50 (NaOH:IPA:DIW), was the only solution used in etching both As_2S_3 and $As_{24}S_{38}Se_{38}$. The etch rate determined for As_2S_3 using that particular etchant was 10.9 ± 2.22 nm/s where for $As_{24}S_{38}Se_{38}$ the etch rate was determined to be 0.360 ± 0.066 nm/s. The difference between the etch rates for these two glasses using this same etchant was ~ 30 fold (30.3). This large difference in etch rates for the two different types of glass with the same etchant suggests a large variation in etchant performance depending on the composition region of the etching substrate. This demonstrates the compositional dependence of the etching process, which can be exploited in designing and fabricating integrated PBG structures.

Abbreviations and Acronyms

ABLC	Grating A, Bottom Left Corner region of Etch 1 Mask
ABRC	Grating A, Bottom Right Corner region of Etch 1 Mask
γ-Al_2O_3	Gamma aluminum oxide
ATLC	Grating A, Top Left Corner region of Etch 1 Mask
ATRC	Grating A, Top Right Corner region of Etch 1 Mask
As_2S_3	Arsenic sulfide (arsenic trisulfide)
$As_{24}S_{38}Se_{38}$	Arsenic sulfide selenide
BBLC	Grating B, Bottom Left Corner region of Etch 1 Mask
BBRC	Grating B, Bottom Right Corner region of Etch 1 Mask
BOE	Buffered oxide etch
BTLC	Grating B, Top Left Corner region of Etch 1 Mask
BTRC	Grating B, Top Right Corner region of Etch 1 Mask
Cr	Chromium
DIW	Deionized water
EMSL	Environmental Molecular Sciences Laboratory
FTM	Film thickness monitor
HF	Hydrofluoric acid
IPA	Isopropyl alcohol or isopropanol
M	Molar (moles per liter)
NaOH	Sodium hydroxide
OH^-	Hydroxide anion
PR	Photoresist
Si	Silicon
SiO2	Silicon dioxide
TF	Tooling factor
UV	Ultraviolet

Contents

1.0 Introduction 1.10

2.0 Experimental Methods 2.11
- 2.1 Summary 2.11
- 2.2 Chromium Deposition 2.14
- 2.3 Batching Etching Solutions 2.15
  - 2.3.1 Batching Stock Solution 2.15
  - 2.3.2 Concentrating Stock Solution 2.16
  - 2.3.3 Diluting Stock Solution 2.17
  - 2.3.4 Making Solutions from Independently Batched 4 M NaOH 2.17
- 2.4 Etching Procedure 2.18

3.0 Results and Discussion 3.20
- 3.1 Arsenic Sulfide (As_2S_3) Results and Discussion 3.20
- 3.2 Arsenic Sulfide Selenide ($As_{24}S_{38}Se_{38}$) Results and Discussion 3.21
- 3.3 Challenges and Observations with Etching Techniques 3.23
  - 3.3.1 Challenge (1): Solubility Restrictions 3.23
  - 3.3.2 Challenge (2): Improperly Prepared Glass Sample Surfaces 3.24
  - 3.3.3 Challenge (3): Irregularities in Chromium Deposit Layer 3.25
  - 3.3.4 Challenge (4): Delamination Issues 3.26
  - 3.3.5 Challenge (5): Inconsistencies in Etching Results 3.29
  - 3.3.6 Challenge (6): Variables in Etching Technique 3.30
  - 3.3.7 Inconsistencies among Etchants 3.33
  - 3.3.8 Analysis of Data for Determining Etch Rate 3.35
- 3.4 Comparing Etching Data Between Glasses 3.22

4.0 Conclusions 4.39

5.0 Acknowledgements 5.40

6.0 References 6.41

Figures

Figure 1. Ribbed waveguide. *A* is a bulk window of As_2S_3, *B* is an overetched $As_{24}S_{38}Se_{38}$ top coating, and *C* is a further top coating of As_2S_3. These three layers, *A*, *B*, and *C* form the bottom clad, core, and top clad, respectively. Light is to be coupled into the core layer via laser. The desired thickness of layer *B*, *h*, is 16 μm. 1.10

Figure 2. Schematic of wet-etching procedure used for chalcogenide glasses. 2.11

Figure 3-A, -B, and -C. Figure 3-A shows a bulk piece of $As_{24}S_{38}Se_{38}$ (BNW14380-031) of which windows were cut. Figure 3-B shows a polished window of $As_{24}S_{38}Se_{38}$. Figure 3-C shows a polished window of As_2S_3. ..... 2.12

Figure 4. Picture of PC-2000 South Bay Technology, Inc. Plasma Cleaner in the Environmental Molecular Sciences Laboratory (EMSL), Laboratory 1321. ..... 2.12

Figure 5. Spincoating device in EMSL cleanroom. 2.13

Figure 6. *Etch 1* FeO mask used to expose all samples on which etch rates were studied. Mask area is a ½" square. Areas of which UV light penetrates to expose sample are white vertical lines. Regions of interest are identified and labeled according to location on mask (i.e., *ATLC*: Grating *A*, Top Left Corner; *BBRC*: Grating *B*, Bottom, Right Corner). 2.13

Figure 7. Exterior of E-beam coater in EMSL 1317 ..... 2.15

Figure 8-A -B and -C. Figure 8-A shows the chemical hood in the EMSL cleanroom. Figure 8-B shows all of the solutions used for chalcogenide glass etching in cleanroom. Figure 8-C shows the chromium etching solution, *Cr-Etch*..... 2.15

Figure 9-A and -B. Schematics demonstrating the differences between chalcogenide etching using traditional Si/SiO_2 methods with a Shipley photoresist as the step-height reference material (Figure 9-A) and using chromium as a step-height reference material (Figure 9-B). The shaded blocks in Figure 9-A represent material that was etched away. 2.18

Figure 22. Data acquired at 4 selected locations for Sample B in using 1:5:10 etchant when determining etch rate. 2.19

Figure 10. Zygo optical profilometer in EMSL 1302 (cleanroom) along with the computers used for analysis of profilometer data collected. Left computer used to find optical fringes on sample view as seen in picture. 2.19

Figure 11. Best fit linear trendline for data etch rate obtained for As_2S_3. ..... 3.20

Figure 12. Linear trendline fit through all $As_{24}S_{38}Se_{38}$ etch rate data points collected for all of the etchants batched. 3.22

Figure 13. Schematic for Si/SiO_2 etching technology. 3.24

Figure 14-A and -B. Figure 14-A shows the data collected from the first tooling factor (TF) calibration sample. Figure 14-B shows a picture of the 8" disc used in the TF calibration procedure where the silicon wafers are masked in regions with green tape. 3.25

Figure 15-A, -B, -C, and -D. Cr-delamination of As_2S_3 thin films upon spincoating. Figure 15-A shows the chromium surface on an As_2S_3 thin film using reflected light as cracked and elevated on the edges. Figure 15-B shows the same sample as in Figure 15-A but using transmitted light which

reveals the cracks around the chromium chunks. Figure 15-C shows a mostly delaminated sample using reflected light and Figure 15-D shows Figure 15-C under a higher magnification..... 3.27

Figure 16-A & -B. Figure 16-A shows chromium delamination from an As_2S_3 sample upon PR-removal that has not yet been subjected to chalcogenide etching. Figure 16-B shows an enlargement of the delamination region in Figure 16-A surrounded by the white dotted line. 3.27

Figure 17-A, -B, -C, -D, -E, and -F. Cr-Delamination of an etched $As_{24}S_{38}Se_{38}$ window from BNW14380-031. Figure 17-A and -B show the grating as elevated locations are covered with chromium which is fractured and delaminating. Figure 17-C and -D show the locations on the sample not covered by gratings undergoing chromium delamination. The dark regions in the pictures are the glass regions and the shining, yellow regions show the presence of the chromium layer as all pictures were taken using reflected light. Figure 17-E and –F show Cr delamination in the darker regions..... 3.28

Figure 18-A, -B, -C, -D, -E, and -F. Comparing optical profilometry of Si/SiO_2-etching system (A, C, E) with chalcogenide-etching system (B, D, F). Figure 18-A, -C, and –E show uniform, definite edges for measuring step-heights, whereas Figure 18-B, -D, and –F show extremely variable, rough, and irregular edges making step-height measurements difficult with any high degree of precision or accuracy. 3.30

Figure 19. Plot of etchant strength over time of etching as the OH^- is neutralized by the glass components (A^+, here)..... 3.32

Figure 20-A -B, -C, and -D. In Figure 20-A, all of the Sample A results are grouped whereas in Figure 20-B, all of the Sample A results are grouped except for the results obtained using the new 1:5:10 etchant. Figure 20-C shows a range of Figure 20-A magnified along with an additional calculated point for the presence of a 3.4:25:50 etchant as it would appear on the Sample A trendline presented there. Figure 20-D is similar to Figure 20-C but the range and calculated data observed is from Figure 20-B. Table 5 compares differences between Sample A and B using the different trendlines to calculate an etch rate for Sample A. 3.34

Figure 21-A, -B, -C, and -D. Optical profilometry of Sample B of $As_{24}S_{38}Se_{38}$ during the 1:5:10(2) etching (see Table 4). The Oblique plot is the three dimensional view of the location where the measurement was taken place and the Profile Plot displays the information regarding the step height, or *yDst*, between the Cr peak and the chalco valley. Figure 21-A, -B, -C, and -D are profilometer readings at 0, 14, 24, & 44 seconds, respectively. 3.36

Figure 23-A, -B, -C, and -D. Plots used in determining concentration needed for desired etch rate..... 3.38

Figure 24-A and -B. Both are Defect-9 PBG Structure. Figure 24-A is a schematic of a structure where 2 μm holes (white) are etched into a chalcogenide substrate (red) and Figure 24-B is a schematic where everything is inverted from Figure 24-A and the majority of the glass is etched down (white) except for rods of residual glass (red)..... 3.23

Equations

$$\alpha_i^e = R_i^e \Big/ \sum_{j=1}^{n} R_j^e \qquad (1) \quad \text{2.16}$$

$$V_i^e = \alpha_i^e V_T^e \qquad (2) \quad \text{2.16}$$

$$m_{4MNaOH} = V_{4MNaOH}^e M_f FW_{NaOH} \text{ (where } M_f = 4mol_{NaOH}/1000mL\text{)} \qquad (3) \quad \text{2.16}$$

$$V_{e_{C,D}}^{(1:25:50)} = V_T^{(e_{C,D})} \alpha_i^{(e_{C,D})} \Big/ \alpha_i^{(1:25:50)} \qquad (4) \quad \text{2.17}$$

$$v_i = V_T^{(e_{C,D})} - V_{e_{C,D}}^{(1:25:50)} \qquad (5) \quad \text{2.17}$$

$$V_i = V_{e_{C,D}}^{(1:25:50)} \alpha_i^{(1:25:50)} \qquad (6) \quad \text{2.17}$$

$$V_i^{(e_{C,D})} = V_i + v_i \qquad \textbf{(7)} \quad \text{2.17}$$

$$E_{time}(u_t) = E_{depth(u_d)} \Big/ \left(R_g\left(u_t/u_d\right)\right) \qquad (8) \quad \text{3.21}$$

$$Tooling\% = TF_i(T_m/T_x) \qquad (9) \quad \text{3.25}$$

$A^+ + OH^- \leftrightarrow A{\cdot}OH$, where $K_c = [A{\cdot}OH]_{eq} / [A^+]_{eq}[OH^-]_{eq}$ (10) 3.31

$$S_{etching} \approx \int_0^{\infty} \frac{1}{\sigma\sqrt{2\pi}} e^{\frac{-(x-\mu)^2}{2\sigma^2}} dx \qquad (11) \quad \text{3.31}$$

$$\Delta yDst = yDst_{max} - yDst_{min} \qquad (12) \quad \text{3.37}$$

$$\Delta t = t_{max} - t_{min} \qquad (13) \quad \text{3.37}$$

$$Etch\ Rate\ (nm/s) = \Delta yDst * \Delta t * 1000 \qquad (14) \quad \text{3.37}$$

Tables

Table 1. Protocol for polishing chalcogenide glass windows. 2.11

Table 2. Entries for FTM used in E-beam chromium vapor depositions. 2.14

Table 3. Chalcogenide glass etching data for As_2S_3. Average is denoted as $R_{As_2S_3}(nm/s)$, standard deviation as σ, and percent deviation as *%Dev*, respectively. Also, As_2S_3 ($g = As_2S_3$) etching times E_{time} (u_t = seconds) required for given etching depth, $E_{depth}(nm)$ = 2000 (u_d = nm), are presented, which were calculated using Equation 11. ..... 3.21

Table 4. Chalcogenide glass etching data for $As_{24}S_{38}Se_{38}$. Under the *Sample used*, *A* refers to 0.75" $As_{24}S_{38}Se_{38}$ disc from BNW14380-031 and *B* refers to 0.98" $As_{24}S_{38}Se_{38}$ disc from November '02, A #8. See Table 3 for explanation of statistical analysis. Also, $As_{24}S_{38}Se_{38}$ etching times (u_t = seconds) required for given etching depth, $E_{depth}(nm)$ = 2000 (u_d = nm), are presented, which were calculated using Equation 11. ..... 3.22

Table 5. Using data acquired for etchants 3.4:25:50 and 1:5:10 to variations in etch rates when using either Sample A or Sample B (see Table 4 and Figure 20-B). 3.34

Table 6. Step height data, or *yDst* (in nm), collected from various locations ($Loc_{\#}$) around the sample at different time intervals on Sample B for 1:5:10 etchant in determination of etch rate. 3.36

Table 7. Summary of data acquired using Sample *B* (see Table 4) for 1:5:10 etchant in determination of etch rate. 3.37

1.0 Introduction

This report describes a study designed to explore the etchability of two different chalcogenide materials, As_2S_3 and $As_{24}S_{38}Se_{38}$, when subjected to photolithographic wet-etching techniques for potential application in fabrication of photonic bandgap (PBG) structures that will function in the long-wave infrared (LWIR) regime. Chalcogenide glasses are made by combining chalcogen elements S, Se, and Te with Group IV and/or V elements.[1] The main goals were to obtain a single variable etch rate curve of etch depth per time versus NaOH overall solution concentration in molarily (M) and to see the difference in etch rate between a given etchant when used on the different chalcogenide stoichiometries. Once generated, these curves can be used in selecting etching conditions for specific stoichiometry and film thickness.

The concentration of sodium hydroxide (NaOH), which Kozicki et al[2] used, is unknown and it is assumed that the ratios stated were batched by volume. The concentration of NaOH arbitrarily chosen for the experiments reported here was a 4 M NaOH solution. When making the etchants for this study, the concentration of 4 M NaOH was altered while keeping the volume ratios of isopropyl alcohol (IPA) and deionized water (DIW) (1:2, respectively). As cited by Kozicki et al,[2] a structure was successfully fabricated with lines and spaces of 35 nm utilizing wet etching methods with an etchant batched using sodium hydroxide (NaOH), IPA and DIW in a ratio of 1:25:50, respectively.

Our future goal is to fabricate and test the structures shown in Figure 1 and Figure 14-A and -B. The etch rates measured in the present task will be used in the fabrication of the structures. The structure seen in Figure 1 utilizes the infrared transparency as well as the high index of refraction inherent in the chalcogenide glass family. As seen in Figure 1, three chalcogenide glass layers, an As_2S_3 bulk glass sample (*A*), an overcoated $As_{24}S_{38}Se_{38}$ thin film (h = 16 µm) which is overetched (*B*), and an As_2S_3 topcoat to backfill the etched trenches (*C*). The layers, *A*, *B*, and *C* function as the top clad, core, and bottom clad in the PBG structure, respectively. A helium-neon (632 nm) or argon (514 nm) laser will be coupled into layer *B* and because of the index of refraction differences between the two glasses, As_2S_3 and $As_{24}S_{38}Se_{38}$, the coupled laser light will be guided through the core $As_{24}S_{38}Se_{38}$ layer.

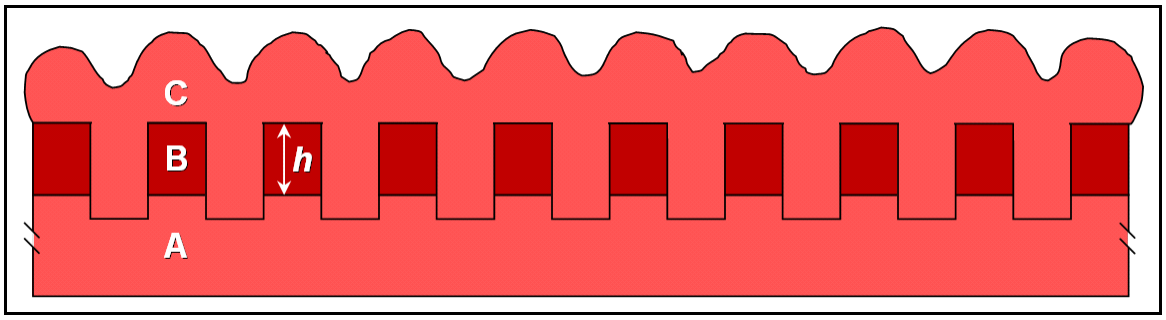

Figure 1. Ribbed waveguide. *A* is a bulk window of As_2S_3, *B* is an overetched $As_{24}S_{38}Se_{38}$ top coating, and *C* is a further top coating of As_2S_3. These three layers, *A*, *B*, and *C* form the bottom clad, core, and top clad, respectively. Light is to be coupled into the core layer via laser. The desired thickness of layer *B*, h, is 16 µm.

2.0 Experimental Methods

2.1 Summary

In order to study the wet-etching properties of As_2S_3 and $As_{24}S_{38}Se_{38}$, much preparation and thought were given to the procedure required to obtain meaningful and accurate data. Many steps were required in the overall process and alterations were made to the procedure during the study to improve certain steps. The overall procedure used in studying the etching rate of a given etchant on these chalcogenide glasses is depicted in Figure 2.

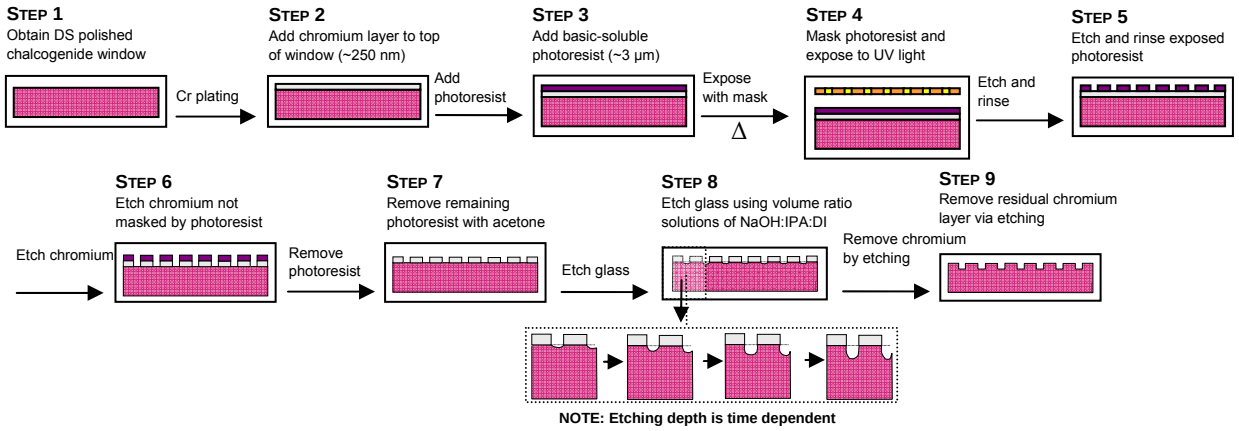

Figure 2. Schematic of wet-etching procedure used for chalcogenide glasses.

From a bulk sample of chalcogenide glass, thin windows were cut to ~ 2.5 mm in thickness using a chalcogenide glass cutting saw and appropriate procedures in the 2400 Stevens, Lab 1230 glovebox using an RPM of ~ 200. Once the windows were cut with two parallel faces, they were polished to a thickness of ~ 2.0 mm in order to satisfy STEP 1 using protocol as seen in Figure 2. Figure 3 shows the pictures of $As_{24}S_{38}Se_{38}$ bulk along with $As_{24}S_{38}Se_{38}$ and As_2S_3 windows. The procedure used in polishing each chalcogenide glass window used in the etching study is summarized in Table 1.

Table 1. Protocol for polishing chalcogenide glass windows.

Step	*Paper/Grit*	*Buehler® solution (µm)*	*Time (sec.)*	*Speed*	*Force*	*Repetitions*
1	600	15	50	35	3	1
2	600	6	50	35	3	1
3	1200	1	180	40	4	2
4	MasterTex®	0.05	180	45	5	2

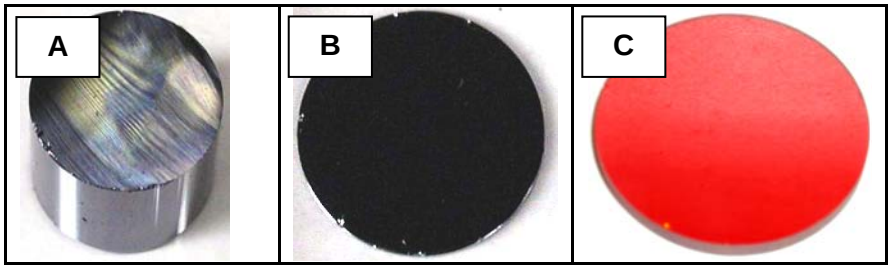

Figure 3-A, -B, and -C. Figure 3-A shows a bulk piece of $As_{24}S_{38}Se_{38}$ (BNW14380-031) of which windows were cut. Figure 3-B shows a polished window of $As_{24}S_{38}Se_{38}$. Figure 3-C shows a polished window of As_2S_3.

Several different cleaning methods were explored for the glass windows and a perfectly effective method is yet to be established. The first method employed a five minute ultrasonicating soak of the sample in acetone followed by a five minute ultrasonicating soak in ethanol. This procedure was later altered where an additional plasma cleaning step was added to the procedure. For the present work, ten minutes of argon plasma cleaning was followed by a ten minute oxygen plasma clean, both with a Forward Power of 40 W. This procedure was adjusted later to three minutes of plasma from each gas along with 10 W of Forward Power with each gas. See Figure 4 for a picture of the plasma cleaner used.

Figure 4. Picture of PC-2000 South Bay Technology, Inc. Plasma Cleaner in the Environmental Molecular Sciences Laboratory (EMSL), Laboratory 1321.

A layer of chromium was applied to the chalcogenide windows in order to satisfy STEP 2 in Figure 2. The thickness of this layer varied from ~ 30-1500 nm between the various depositions performed using the coater in EMSL 1317 (see Figure 7). The Cr-layer was followed by the application of ~ 5 mL of Shipley 1818, a photoresist (PR), for STEP 3. Once the PR was applied via spincoating at 2400 revolutions per minute for 30 seconds, the sample was set to bake on a hotplate enduring a 20°C to 85°C ramp heat over a 20 minute time interval to soak for 2 minutes and then slow cool to room temperature.

Figure 5. Spincoating device in EMSL cleanroom.

In STEP 4 of Figure 2, after the PR was baked, it was exposed via ultraviolet light for 99.9 seconds using a mask to selectively expose the PR. The mask used in all of these experiments is the *Etch 1* mask as seen in Figure 6. *Etch 1* has a few strategically different features, masked and unmasked regions as well as two different sets of gratings, *A* (100 sub-gratings) and *B* (30 sub-gratings), both included in Figure 6. The unmasked regions are 40 µm across and the masked regions are 60 µm across. Gratings *A* and *B* are separated by a 300 µm gap. The eight different regions of interest on the samples exposed by the mask are labeled in Figure 6. These regions were chosen because they were easy to reference on the sample due to their location being on the corners of the different gratings. Following sample exposure, the exposed PR was removed using MF-321 solution in STEP 5 of Figure 2, leaving surface contour on the sample analogous to the *Etch 1* mask.

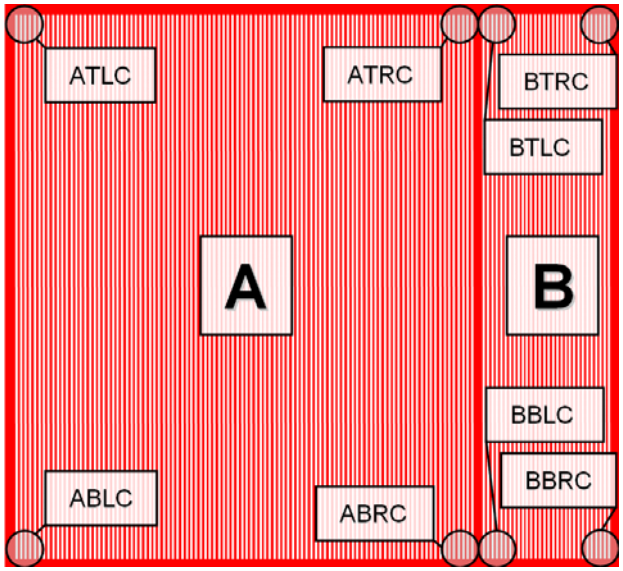

Figure 6. *Etch 1* FeO mask used to expose all samples on which etch rates were studied. Mask area is a ½" square. Areas of which UV light penetrates to expose sample are white vertical lines. Regions of interest are identified and labeled according to location on mask (i.e., *ATLC*: Grating *A*, Top Left Corner; *BBRC*: Grating *B*, Bottom, Right

Corner).

The exposed chromium layer not top-coated by PR, was etched in STEP 6 of Figure 2 using a mixture of HNO_3, $(NH_4)_2Ce(NO_3)_6$,[3] and DIW and was labeled as *Cr-Etch* (see Figure 8-C). In STEP 7, once the chromium not top-coated by PR was fully etched all the way to the glass as seen in STEP 6 which was determined using optical microscope with transmitted light and when $\Delta yDst = 0$ (see Figure 23) the PR layer was removed using acetone.[i]

Once these previous steps, STEP 1 - STEP 7, have been completed, the chalcogenide glass etching step, STEP 8, was performed using solutions containing specific volume ratios of sodium hydroxide (NaOH), IPA, and DIW. The IPA:DIW ratio was fixed at 1:2 and the volume of 4 M NaOH was adjusted in different ratios to the DIW and IPA in order to achieve different, specific overall NaOH concentrations.

In order to observe the chalcogenide glass etching progress, a Zygo optical profilometer was used in the EMSL cleanroom. A *zero* measurement was made (pre-etched sample) and as the chalcogenide glass was etched in small time intervals (5-20 seconds), proceeding measurements were made with the profilometer (see Figure 9-B). For an accurate overall summary, various different regions on each sample were analyzed (see Figure 6) in order to detect an increase in overall step height using the entire sample region between the top of the chromium layer peak and the bottom of the chalcogenide glass valley on the profilometer readout (h_f in Figure 9-B*3*). Step height was defined as the vertical height difference between two layers (see Figure 14). In STEP 9, once the chalcogenide etching was completed and the sample was ready for further testing, the chromium layer was removed using the *Cr-Etch* solution seen in Figure 8-C.

2.2 Chromium Deposition

The E-beam evaporative coater in EMSL 1317 was used to perform the vapor depositions of chromium which was used for masking the chalcogenide glass surfaces. To perform these depositions, an 8" diameter metal disc (see Figure 16-B) was secured with samples to be deposited on and the disc was load into the chamber onto shaft-1 of a double planetary rotation device capable of holding three discs at once. On the disc, masked silicon wafers were added at specific distances from the center of the disc for step-height verification upon deposition completion via the Zygo non-contact optical profilometer in EMSL 1302. An Inficon film thickness monitor (FTM) was used to determine the film thickness while deposition was occurring. The values used for the FTM during deposition are found in Table 2. The Tooling Factor (TF) values were variable due to incorrect provided values (see Figure 16). A picture of the E-beam coater's external is seen in Figure 7.

Table 2. Entries for FTM used in E-beam chromium vapor depositions.

Entry	Value
Tooling Factor	40-70%
Z-ratio	0.305
ρ_{Cr}	7.200 g/cm^3

[i] It is difficult to determine when the chromium etching is complete due to the low transmission of visible light through the $As_{24}S_{38}Se_{38}$ glass. Also, the chromium appears to be transparent when very thin, appearing to be completely etched away.

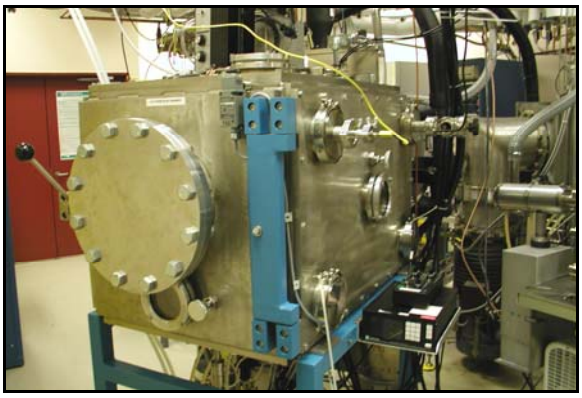

Figure 7. Exterior of E-beam coater in EMSL 1317

2.3 Batching Etching Solutions

In creating the etching solutions, STEP 8 as seen in Figure 2, three different methods were used: batching up a stock solution, using the stock solution to make more concentrated solutions, and using the stock solution to make more dilute solutions. The idea for the stock solution was found in the literature as a 1:25:50 volume ratio solution of NaOH:IPA:DIW, respectively. The concentration of NaOH to use was not known for certain so a 4 M NaOH concentration was chosen. When new solutions needed to be made, at first the stock solution was either diluted or concentrated with more 4 M NaOH to the desired ratio to the IPA and DIW already present, but the ratio of IPA:DIW was held constant at 1:2 throughout all of the etching studies performed. Figure 8-B shows all of the chalcogenide etchants used which are stored on a shelf in the EMSL cleanroom and Figure 8-C shows the *Cr-Etch* solution.[ii]

Figure 8-A -B and -C. Figure 8-A shows the chemical hood in the EMSL cleanroom. Figure 8-B shows all of the solutions used for chalcogenide glass etching in cleanroom. Figure 8-C shows the chromium etching solution, *Cr-Etch*.

2.3.1 Batching Stock Solution

The 1:25:50 (4 M NaOH:IPA:DIW) stock solution was batched using volume fractions for each component as determined via Equation 1. In Equation 2**,** α_i^e is the volume fraction of *i*-th solution

[ii] All etching was performed in the EMSL Cleanroom, lab 1306, along with all of the etchant preparation except batching of the stock solution (1:25:50 volume ratios of 4 M NaOH:IPA:DIW) and the 4 M NaOH; the 4 M NaOH here was used in making 1:5:10(3) etchant. All of the chalcogenide glass cutting and polishing was performed in the chalcogenide glass handling glovebox in 2400 Stevens lab 1230. The plasma cleaning was performed in EMSL, lab 1321. All chromium coating was done so using the E-beam evaporative coater in EMSL lab 1317. All of the optical profilometry was performed using the Zygo profilometer in the EMSL Cleanroom, lab 1302.

component in etchant *e*, R_i^e is the ratio value for the *i*-th solution component in etchant *e*, and $\sum_{j=1}^{n} R_j^e$ is the sum of the ratio values of all solution components in etchant *e* (i.e., the value for *e* when working with the stock solution as the etchant is 1:25:50).[iii]

Once α_i^e was determined for each solution component, *i*, Equation 2 was used to determine the volume required of each component, V_i^e, where V_T^e was the total solution volume desired.[iv] When adding the 4 M NaOH component of the solution, $V_{4MNaOH}^{(1:25:50)}$, it was batched on-the-fly[v] as needed to minimize waste.

$$\alpha_i^e = R_i^e \Big/ \sum_{j=1}^{n} R_j^e \quad \textbf{(1)}$$

$$V_i^e = \alpha_i^e V_T^e \quad \textbf{(2)}$$

Since the 4 M NaOH was batched on-the-fly, in order to determine the mass of NaOH, m_{4MNaOH}, powder required for the mixture, Equation 3 was used where $V_{4MNaOH}^{(1:25:50)}$ was determined in Equation 1, M_f is the molarity conversion factor, and FW_{NaOH} is the formula weight of NaOH (39.99711 $^{g}/_{mol}$ was used here). Once the V_i^e values were known for all components along with the value of m_{4MNaOH}, the etchant was batched accordingly. Once the stock solution of 1:25:50 was used on both As_2S_3 and $As_{24}S_{38}Se_{38}$, new etchants were made according to the etch rate response. To increase or decrease the strength of the stock etchant, the concentration of NaOH present in the etchant was either increased or decreased, respectively.

$$m_{4MNaOH} = V_{4MNaOH}^e M_f FW_{NaOH} \text{ (where } M_f = 4mol_{NaOH}/1000mL\text{)} \quad \textbf{(3)}$$

2.3.2 Concentrating Stock Solution

To increase the strength of the stock etchant for use with $As_{24}S_{38}Se_{38}$, the concentration of NaOH present in the etchant was increased. To begin this process, the stock solution was further concentrated by adding more 4 M NaOH in the desired proportion while leaving $V_{IPA}^{(e_C)}$ and $V_{DI}^{(e_C)}$ constant where e_C was substituted for *e* as the more concentrated etchant in comparison to the stock solution. The first etchant made that was more concentrated than the stock solution was the 1:1:2 volume ratio solution. To calculate the volume of the stock solution to start with prior to concentrating, $V_{e_C}^{(1:25:50)}$, in order to obtain a

---

[iii] The ratio of components for the stock solution is 1:25:50 (4 M NaOH:IPA:DIW). For all components in the 1:25:50 etchant, $\sum_{j=1}^{n} R_j^{(1:25:50)} = 76$, and for 4 M NaOH, $R_i^{(1:25:50)} = R_{4MNaOH}^{(1:25:50)} = 1$, therefore, $\alpha_{4MNaOH}^{(1:25:50)} = 0.01316$.

[iv] Since a 500 mL batch of stock solution was made, $V_T^{(1:25:50)} = 500$ mL and $\alpha_{4MNaOH}^{(1:25:50)} = 0.01316$, therefore $V_i^e = V_{4MNaOH}^{(1:25:50)} = 6.579$ mL.

[v] Instead of adding a volume quantity of 4 M NaOH, the proper amount of 4 M NaOH was added to the stock solution by adding the required amount of NaOH powder along with the correct amount of DIW to dissolve the NaOH to make it a 4 M solution of NaOH.

desired total volume, $V_T^{(e_C)}$, along with the desired volume ratios from e_C, where here, e_C is 1:1:2 (volume ratios of 4 M NaOH, IPA, and DIW, respectively), Equation 4 was used.[vi]

Once the value of $V_{e_C}^{(1:25:50)}$ was calculated, the additional volume of 4 M NaOH required to complete the solution, v_{4MNaOH}, was calculated using Equation 5. Equation 6 provides a way of calculating the total volume of component i in the stock solution, where here, i is 4 M NaOH. Using Equation 5 and Equation 6, Equation 7 was used to verify that the total volume of 4 M NaOH in the new concentrated etchant, $V_{4MNaOH}^{(e_C)} = V_T^{(e_C)}\alpha_{4MNaOH}^{(e_C)}$. Using the value of v_{4MNaOH} obtained using Equation 5, m_{4MNaOH} can be calculated using Equation 3**,** which is to be added to a quantity of water equal to v_{4MNaOH}.

$$V_{e_{C,D}}^{(1:25:50)} = V_T^{(e_{C,D})}\alpha_i^{(e_{C,D})} \Big/ \alpha_i^{(1:25:50)} \quad \textbf{(4)}$$

$$v_i = V_T^{(e_{C,D})} - V_{e_{C,D}}^{(1:25:50)} \quad \textbf{(5)}$$

$$V_i = V_{e_{C,D}}^{(1:25:50)}\alpha_i^{(1:25:50)} \quad \textbf{(6)}$$

$$V_i^{(e_{C,D})} = V_i + v_i \quad \textbf{(7)}$$

2.3.3 Diluting Stock Solution

To decrease the strength of the stock etchant for use on As_2S_3, the concentration of NaOH present in the etchant was decreased. To begin this process, the stock solution was diluted by adding more IPA:DIW in a 1:2 volume ratio in the desired proportion while leaving $V_{4MNaOH}^{(e_D)}$ constant where e_D is the more diluted etchant. The first etchant made that was more dilute than the stock solution was the 1:50:100 volume ratio solution. Equation 4 was used to calculate the volume of the stock solution to start with prior to diluting, $V_{e_D}^{(1:25:50)}$, in order to obtain a desired total volume, $V_T^{(e_D)}$, along with the desired volume ratios from e_D, where here, e_D is 1:50:100 (volume ratios of 4 M NaOH, IPA, and DIW, respectively). Once $V_{e_D}^{(1:25:50)}$ was calculated, the additional volumes of IPA, v_{IPA}, and DIW, v_{DIW}, required to complete the solution were calculated using Equation 5. When diluting, Equation 6 was used to calculate the total volume of component i in the stock solution, where here, i is substituted for both IPA and DI, separately. Using Equation 5 and Equation 6, Equation 7 was used to verify that the total volumes of IPA, $V_{IPA}^{(e_D)}$, and DIW, $V_{DIW}^{(e_D)}$, in the new concentrated etchant were equal to $V_T^{(e_D)}\alpha_{IPA}^{(e_D)}$ and $V_T^{(e_D)}\alpha_{DIW}^{(e_D)}$, respectively.

2.3.4 Making Solutions from Independently Batched 4 M NaOH

In order to make the stock solution and a newly batched 1:5:10(3) etchant along with an unused 3.4:25:50 etchant, a fresh 50 mL batch of 4 M NaOH was made in order to make etchants up by simply mixing the 4 M NaOH solution with IPA and DIW in the desired ratios to get a different solution. To batch the 4 M

[vi] If i = DI, then $\alpha_i^{(1:25:50)} = \alpha_{DI}^{(1:25:50)} = 0.6579$ and since e_C = 1:1:2, $\alpha_i^{(e_C)} = \alpha_{DI}^{(1:1:2)} = 0.5$. Therefore, if $V_T^{(e_C)} = 50$ mL, $V_{e_C}^{(1:25:50)} = 38$ mL.

NaOH solution, Equation 3 was used where V^{e}_{4MNaOH} = 50 mL. The data acquired from the 1:5:10(3) etchant is found in Table 3.

2.4 Etching Procedure

Once each sample was prepared via STEP 1 – STEP 7 in Figure 2, the etch rate study began. Initial step height measurements were made between the top of the chromium ridge and the top, exposed surface of the chalcogenide glass window where the chromium was etched away (see STEP 6 of Figure 2), using the Zygo non-contact profilometer in the cleanroom. The resulting original step height measurements were referred to as ref_0 measurements as seen in Figure 9-A and -B.

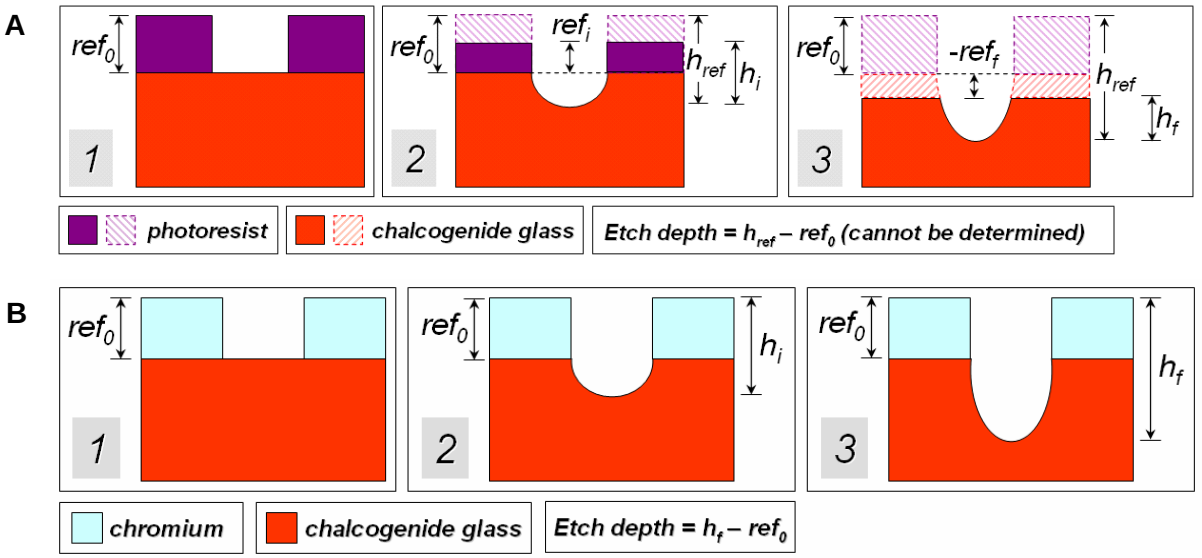

Figure 9-A and -B. Schematics demonstrating the differences between chalcogenide etching using traditional Si/SiO_2 methods with a Shipley photoresist as the step-height reference material (Figure 9-A) and using chromium as a step-height reference material (Figure 9-B). The shaded blocks in Figure 9-A represent material that was etched away.

As mentioned previously, these ref_0 values were obtained in as many regions on the sample, which could be relocated for repeatable measurements in at least eight regions, as seen in Figure 6. The sample was soaked in the desired wet etchant for short time intervals (5-20 seconds), the sample was rinsed in DIW to remove the etchant, and then the new step height was measured using the profilometer in duplicate or triplicate. These new values were recorded as h_i values (or *height-at-interval* values) as seen in Figure 9-B*2*. After data was collected at several time intervals where h_f, the final step-height value, was determined, the data was analyzed (Figure 9-B*3*). As seen in Figure 9-B*3*, the value of h_f - ref_0 is equal to the etch depth of an etchant. This data was collected at each of the locations seen in Figure 6, compared against the duration of the etching procedure, and the etch rate was determined from the slope of the linear trendline as seen in Figure 10.

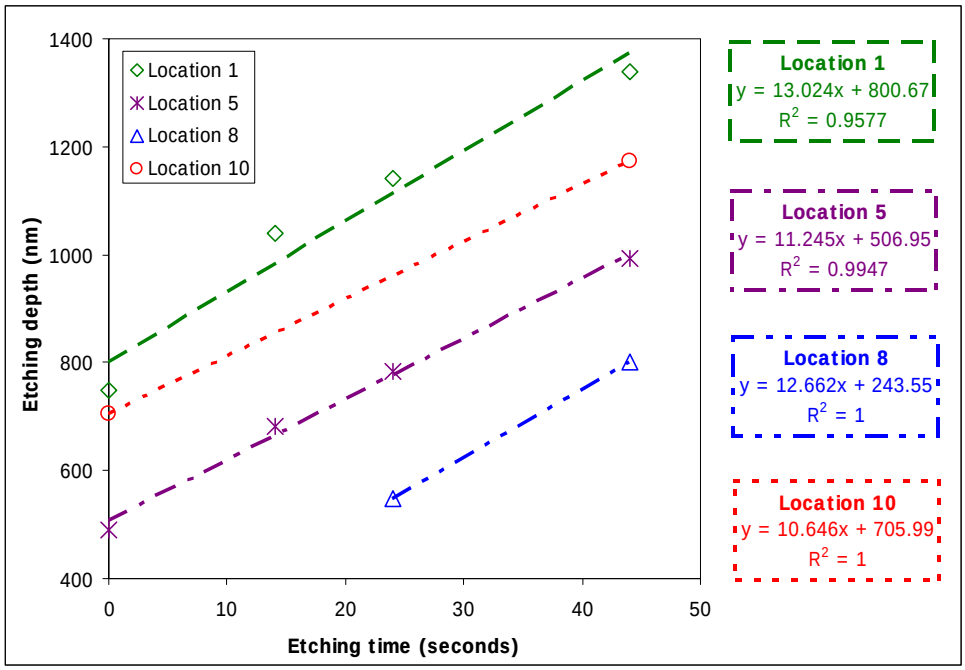

Figure 10. Data acquired at 4 selected locations for Sample B in using 1:5:10 etchant when determining etch rate.

See Figure 11 for a picture of the profilometer and accompanying computers used for data analysis of the information obtained. The x-y stage location and tilt were controlled using the joysticks connected to the computer in the center of Figure 11. The fringe pattern can be seen on the computer in the middle of the screen.

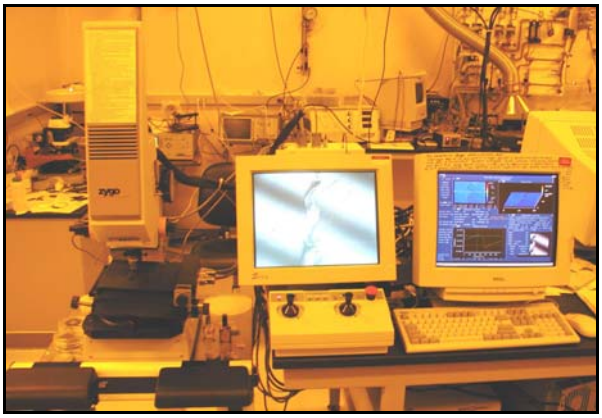

Figure 11. Zygo optical profilometer in EMSL 1302 (cleanroom) along with the computers used for analysis of profilometer data collected. Left computer used to find optical fringes on sample view as seen in picture.

3.0 Results and Discussion

For data analysis, some statistical calculations were made for aid in comparison of the masses of data collected and calculated. The average, $\bar{x}$, standard deviation, $\sigma = \sqrt{\frac{n\sum x^2 - \left(\sum x\right)^2}{n(n-1)}}$, and percent deviation $\%Dev = 100\left(\sigma/\bar{x}\right)$, were used to compare all of the etching results. Upon etching the chalcogenide glass samples, a positive correlation was observed between the NaOH overall solution concentration and the strength of the etchant as defined by etch rate results.

3.1 Arsenic Sulfide (As_2S_3) Results and Discussion

As seen in Table 3, the etching rate varied widely for different overall concentrations of 4 M NaOH from 0.984 ± 0.055 nm/s for 1:100:200 solution (NaOH:IPA:DIW), the most dilute solution with an overall NaOH concentration of 0.013 M, to 10.9 ± 2.22 nm/s for 1:25:50 solution with an overall NaOH concentration of 0.053 M, the most concentrated of the etchants used for As_2S_3. See Figure 13 for graphical representation of data in Table 3.

In observation of data for As_2S_3, a linear trendline in Figure 12 fits nicely with a high correlation coefficient of $R^2 = 0.999$. This high correlation coefficient to a linear trendline suggests that the etch rate and concentration of NaOH share a linear relationship for As_2S_3, at least in this narrow concentration range (0.013 M to 0.053 M overall NaOH concentration).

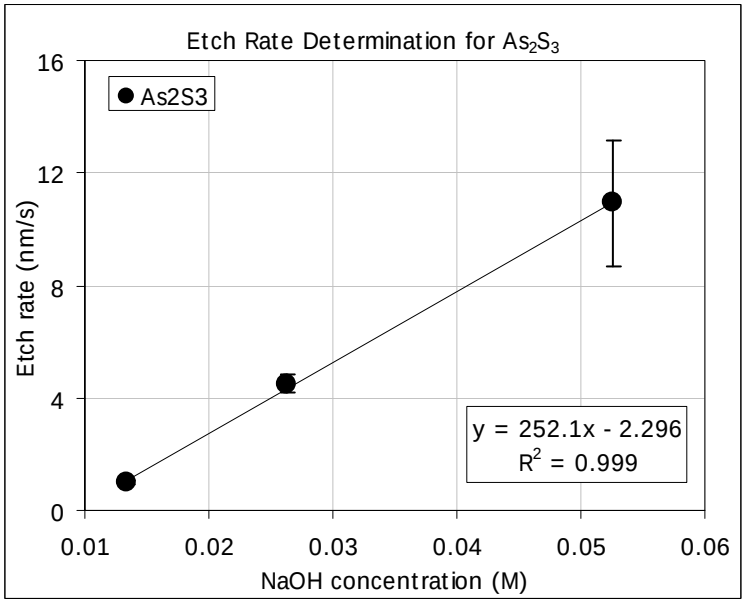

Figure 12. Best fit linear trendline for data etch rate obtained for As_2S_3.

Using Equation 11, the etching time in time units, u_t, $E_{time}(u_t)$, required for a particular etching depth, $E_{depth(u_d)}$, using an etchant with a known etching rate for a given chalcogenide glass, R_g, with units of u_t/u_d, can be calculated. Using Equation 11, Table 3 was made using a theoretical $E_{depth}(nm)$ of 2000 nm (or 2 μm) and the corresponding $E_{time}(s)$ required.

$$E_{time}(u_t) = E_{depth(u_d)} / \left(R_g(u_t / u_d)\right) \quad \textbf{(8)}$$

Table 3. Chalcogenide glass etching data for As_2S_3. Average is denoted as $R_{As_2S_3}(nm/s)$, standard deviation as σ, and percent deviation as *%Dev*, respectively. Also, As_2S_3 (g = As_2S_3) etching times E_{time} (u_t = seconds) required for given etching depth, $E_{depth}(nm)$ = 2000 (u_d = nm), are presented, which were calculated using Equation 11.

Etchant	*NaOH(M)*	$R_{As_2S_3}(nm/s)$	*σ (nm/s)*	*%Dev. (nm/s)*	$E_{time}(s)$
1:100:200	0.013	0.984	0.055	5.62	2033
1:50:100	0.026	4.496	0.315	7.00	444.8
1:25:50	0.053	10.926	2.219	20.3	183.1

Some of the data acquired during the chalcogenide etching is not totally accurate but it will be used to estimate required etch time needed for a specifically desired etch depth using a particular etchant on a given glass. Chromium delamination was experienced while etching bulk and thin film samples of As_2S_3 as seen in Figure 17 and Figure 18.

3.2 Arsenic Sulfide Selenide ($As_{24}S_{38}Se_{38}$) Results and Discussion

As seen in Table 4, the etching rate varied widely for different overall concentrations of NaOH from 0.360 ± 0.066 nm/s for 1:25:50 solution (4 M NaOH:IPA:DIW), the most dilute solution with an overall NaOH concentration of 0.0526 M to 120 ± 7.02 nm/s for 1:1:2 solution with an overall NaOH concentration of 0.980 M, the most concentrated of the etchants used for $As_{24}S_{38}Se_{38}$. See Figure 15 for graphical representation of data in Table 4.

In observation of the data acquired for $As_{24}S_{38}Se_{38}$ glass etching, a linear trendline did not fit accordingly under the full concentration region studied – see Figure 13. Because the data did not fit a linear trendline, second and third order trendlines were fit to various different sets of the data separated by glass sample used, etchant preparation method used, and calculated data compared with the measured data. As was done for As_2S_3, using Equation 11, Table 4 was made for $As_{24}S_{38}Se_{38}$ data using a theoretical $E_{depth}(nm)$ of 2000 nm (or 2 μm) and the corresponding $E_{time}(s)$ required.

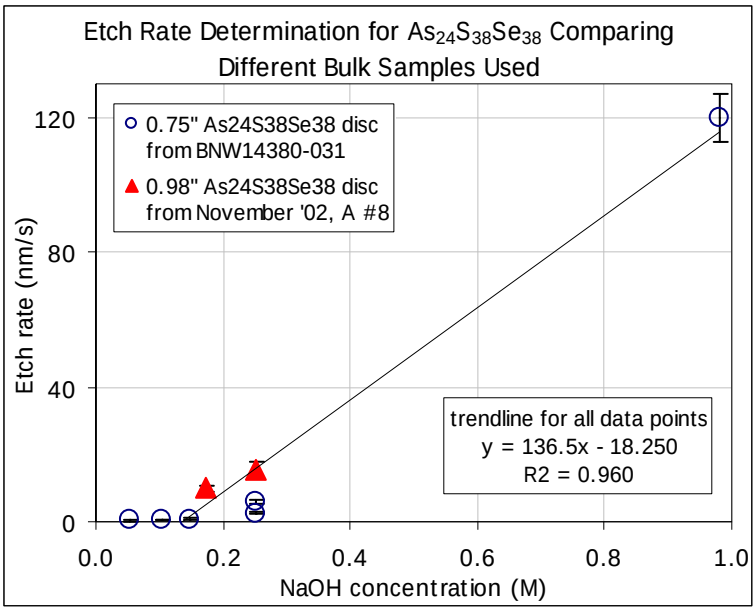

Figure 13. Linear trendline fit through all $As_{24}S_{38}Se_{38}$ etch rate data points collected for all of the etchants batched.

Table 4. Chalcogenide glass etching data for $As_{24}S_{38}Se_{38}$. Under the *Sample used*, *A* refers to 0.75" $As_{24}S_{38}Se_{38}$ disc from BNW14380-031 and *B* refers to 0.98" $As_{24}S_{38}Se_{38}$ disc from November '02, A #8. See Table 3 for explanation of statistical analysis. Also, $As_{24}S_{38}Se_{38}$ etching times (u_t = seconds) required for given etching depth, $E_{depth}(nm) = 2000$ (u_d = nm), are presented, which were calculated using Equation 11.

Etchant	*NaOH(M)*	$R_{As_{24}S_{38}S_{38}}(nm/s)$	σ	*%Dev.*	$E_{time}(s)$	*Sample used*
1:25:50	0.0526	0.3597	0.0663	18.43	5561	A
2:25:50	0.1039	0.3989	0.0720	18.05	5014	A
2.94:25:50	0.1472	0.7837	0.1087	13.87	2552	A
3.4:25:50	0.1735	9.988	0.971	9.72	200.2	B
1:5:10 (1)	0.2500	5.777	0.458	7.93	346.2	A
1:5:10 (2)	0.2500	15.52	2.56	16.49	128.8	B
1:5:10 (3)	0.2500	2.592	0.510	19.66	771.6	A
1:1:2	0.9804	119.9	7.0	5.85	16.69	A

3.3 Comparing Etching Data Between Glasses

The data for etching As_2S_3 and $As_{24}S_{38}Se_{38}$, found in Table 3 and Table 4, varies extensively. The stock etchant, 1:25:50, was the only solution used in etching both As_2S_3 and $As_{24}S_{38}Se_{38}$. The etch rate determined for As_2S_3 using that particular etchant was 10.9 ± 2.22 nm/s where for $As_{24}S_{38}Se_{38}$ the etch rate was determined to be 0.360 ± 0.066 nm/s. The difference between the etch rates for these two glasses using this same etchant was ~ 30 fold (30.3). This large difference in etch rates for the two different types of glass with the same etchant suggests a large variation in etchant performance depending on the composition region of the etching substrate. The differences between the two glasses used here are: [1)]$As_{24}S_{38}Se_{38}$ contains the much heavier element, selenium, where As_2S_3 does not, [2)]$As_{24}S_{38}Se_{38}$ has smaller mole fraction of arsenic [3)]as well as sulfur than does As_2S_3. The addition of Se to the As-S system leads to stronger structural bonding and thus a lower etching rate. This demonstrates the compositional

dependence of the etching process. This difference can also exploited in designing and fabricating integrated PBG structures as seen in Figure 14.

For Figure 14-A, a series of holes (seen in white) will be etched in a bulk chalcogenide glass sample. Figure 14-B, the majority of a chalcogenide glass sample is etched down except for residual rods. A laser will be coupled into the bend *defect* in both instances utilizing the change in index of refraction to keep the laser light coupled into the desired path. The primary difference between the structures in Figure 14-A and Figure 14-B is that the chalcogenide glass will be waveguide in Figure 14-A where the waveguide will be the air surrounding the glass in Figure 14-B.

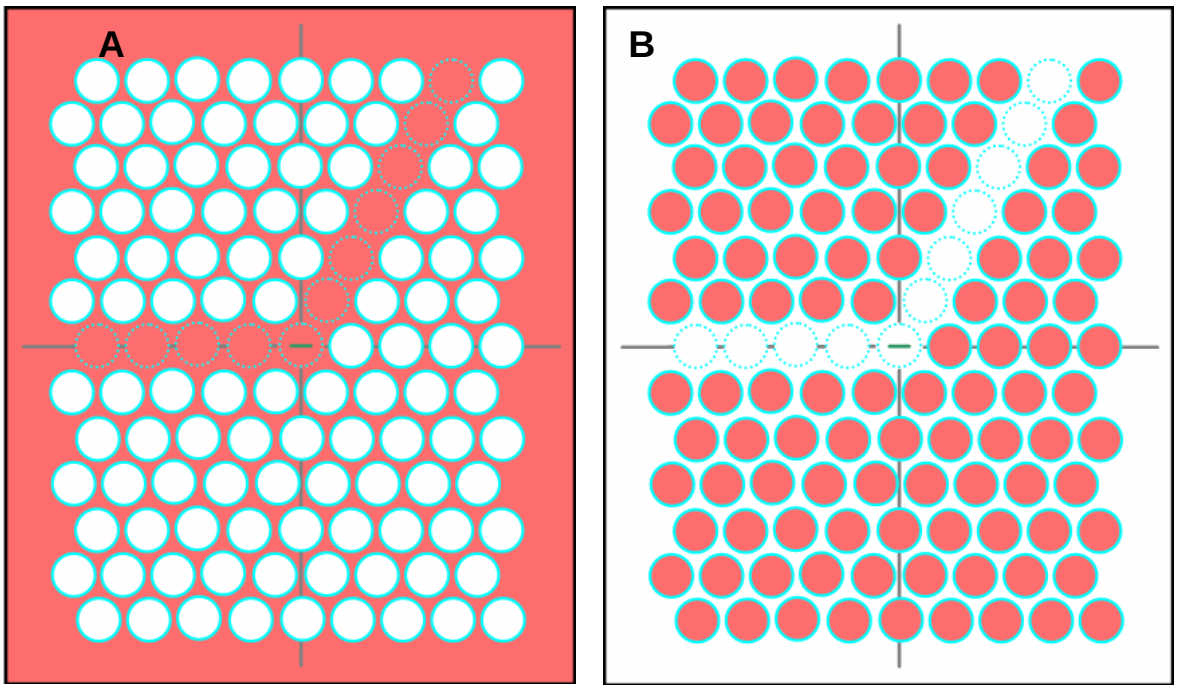

Figure 14-A and -B. Both are Defect-9 PBG Structure. Figure 14-A is a schematic of a structure where 2 μm holes (white) are etched into a chalcogenide substrate (red) and Figure 14-B is a schematic where everything is inverted from Figure 14-A and the majority of the glass is etched down (white) except for rods of residual glass (red).

3.4 Challenges and Observations with Etching Techniques

Several Challenge(s) were encountered during the etching studies including:

(1) Solubility restrictions
(2) Improperly prepared glass sample surfaces
(3) Irregularities in chromium deposit layer
(4) Delamination of the different layers during processing
(5) Inconsistencies in etching results
(6) Variables in etching technique

These challenges are discussed in the following section.

3.4.1 Challenge (1): Solubility Restrictions

In regards to Challenge (1), solubility restrictions, the first barriers introduced in the etching study were the solubility of the components being used. One of the best known procedures for semiconductor

photolithography is that involving silicon and silicon dioxide along with a basic-soluble PR as seen in Figure 15 where procedures such as STEP(s) 3, 4, and 5 in Figure 2 are similarly performed. As in PHASE 1, the typical procedure involves baking a silicon wafer in an O_2-rich environment which results in the controlled growth of an oxide layer diffusing into the silicon structure creating a uniform glassy silica layer on top of the silicon substrate. The wafer is then cut in PHASE 2, and then a basic-soluble PR such as Shipley 1818 is spincoated over the wafer which is baked in PHASE 3. In PHASE 4 the wafers are exposed with a mask, and rinsed in PHASE 5, uncovering a patterned region of SiO_2. SiO_2 glass, being soluble in hydrofluoric acid, can be etched uniformly without modifying the PR layer as in PHASE 6 which is followed by PHASE 7, an acetone rinse to remove the PR. The biggest problem in the etching study was learned during an important realization: this same Si/SiO_2 technology could not be used on chalcogenide glass substrates due to the fact that along with the best commercially available PR materials, chalcogenide glass is also basic-soluble. See Figure 9-A for schematic of the results upon chalcogenide glass etching using traditional Si/SiO_2 etching methods.

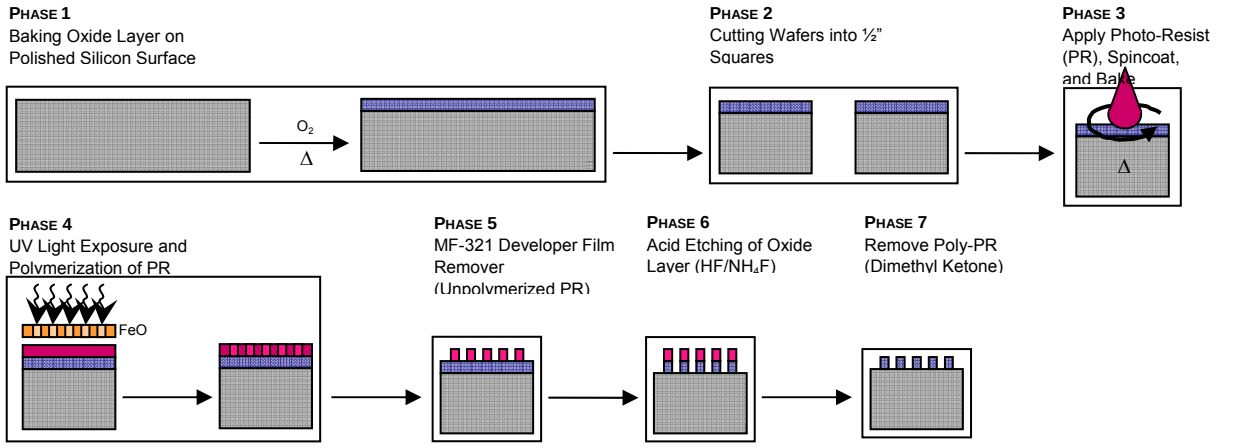

Figure 15. Schematic for Si/SiO_2 etching technology.

When performing etch rate studies, the only way to determine the achieved etch depth is to have a reference point, a role generally held by the photoresist. Due to the like-solubility of the Shipley PR and chalcogenide glasses, a new approach had to be taken. Utilizing a suggestion by Dr. Laxmikant Saraf, an acid-soluble, a basic-insoluble chromium layer, which could be patterned using an overcoated PR layer (see Figure 2, STEP 2 – STEP 7), was used. This was a good way to utilize the solubility dissimilarities of the different materials being used as the chromium would survive the chalcogenide glass etching and result in a static step-height reference material as seen in Figure 9-B. Using this different, less well-known procedure, resulted to more, unexpected problems (e.g., delamination of the chromium layer).

3.4.2 Challenge (2): Improperly Prepared Glass Sample Surfaces

Regarding Challenge (2), improperly prepared glass sample surfaces, the polishing performed on the chalcogenide glass surface was regarded as insufficient (see Table 1). Upon inspection of the windows after this polishing process was completed via optical microscopy, micron and submicron scratches were observed. Future planning included an alteration to the procedure by performing further polishing steps with finer grit polish (γ Al_2O_3) in order to remove the submicron scratches from the glass surface. This step has yet to be implemented because all of the samples used in this study for testing were prepared prior to the implementation of this new procedure.

3.4.3 Challenge (3): Irregularities in Chromium Deposit Layer

In analysis of Challenge (3), irregularities in chromium deposit layer or masking layer thickness variability, the chromium layer applied using the E-beam evaporative coater in EMSL/1317 varied in thickness as well as uniformity. The thickness variability is mostly due to the fact that the tooling factor (TF) for the film thickness monitor (FTM) was never calibrated properly for usage of chromium in E-beam depositions using that particular chamber due to time and funding constraints. The substrate present in the chamber for targeted deposition is located on a double planetary rotation platform inside the chamber. Since the source crucible emitting the chromium condensate is at a different distance from the crystal, $D_{crystal}^{crucible}$, than it is from the substrate, $D_{substrate}^{crucible}$, the data collected by the FTM crystal is inherently a different coating rate and thickness than the substrate. The TF simply corrects for this difference.

As seen in Table 2, the TF settings used in performing the various depositions varied over a large range (40-70%). Changing this value resulted in an extensive variance between the FTM reading for film thickness upon completion of a deposition, T_x, and the actual thickness, T_m, as verified via the profilometer. The procedure for calculating the TF involves a series of depositions to narrow the range in determination of the value. Using Equation 8, the starting value for TF_i, the initial TF %, was 100. This value was entered into the FTM for the initial deposition. Once values for T_m and T_x were attained and the *Tooling*% is calculated, then for the next deposition, the new TF_i value entered was the value *Tooling*% calculated using data from the previous deposition. To further identify the precise value of the TF, several depositions were required; the more depositions performed, the more precise the Tooling Factor, or *Tooling*%, will be.

$$Tooling\% = TF_i(T_m/T_x) \quad \textbf{(9)}$$

The initial TF calibration results are found in Figure 16. As seen from Figure 16, the TF values arbitrarily chosen for the previous chromium E-beam depositions (40-70%) were near the actual TF, which, thus far, is determined to be ~ 56.10.

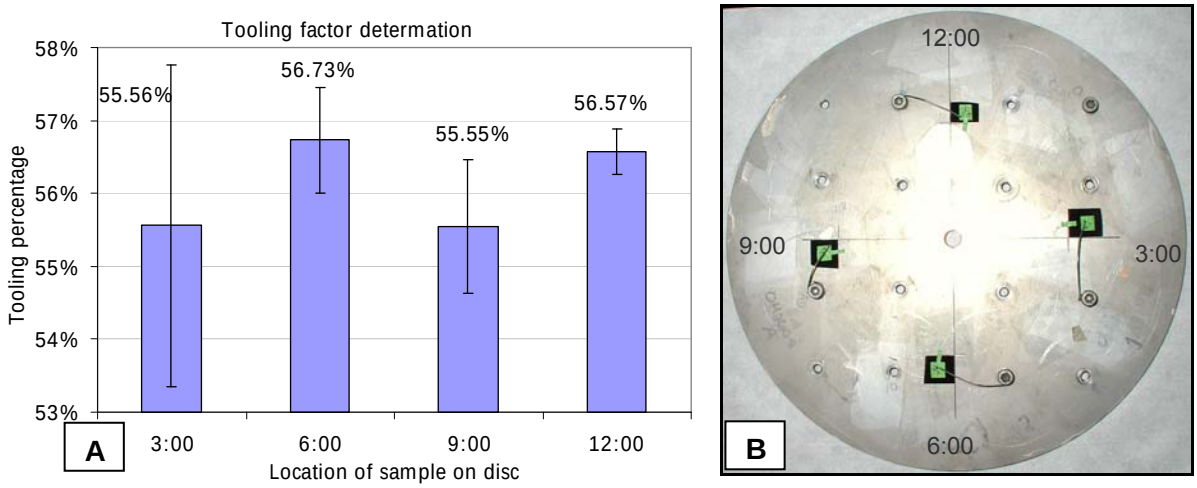

Figure 16-A and -B. Figure 16-A shows the data collected from the first tooling factor (TF) calibration sample. Figure 16-B shows a picture of the 8" disc used in the TF calibration procedure where the silicon wafers are masked in regions with green tape.

3.4.4 Challenge (4): Delamination Issues

In analysis of Challenge (4), the delamination of the various chemical component layers involved, including: As_2S_3 thin film and chromium delamination upon spincoating an As_2S_3-coated fused quartz substrate (Figure 17) and chromium delamination from As_2S_3 pre-etched bulk windows (Figure 18) and $As_{24}S_{38}Se_{38}$ etched bulk windows (Figure 19). Initial delamination occurred with the first etching of a chalcogenide glass layer. While overcoated with PR, the chromium appears to stay intact for chromium etching (Figure 2, STEP 6), but as soon as the PR was removed and the entirety of the chromium exposed, the chromium seemed to be affected via some magnitude of delamination by all of the chalcogenide etchants. This could mean that as well as being acid-soluble, chromium is mildly basic-soluble.

In Figure 17, chromium delamination from As_2S_3 pre-etched bulk windows is seen. A thin film (4 μm) of As_2S_3 was applied to fused quartz ½" squares. These quartz squares were top-coated with chromium and then they were spincoated. During spincoating, the chromium layer was delaminated, either partially or completely. As seen in Figure 17-A using reflected light, the chromium surface on this partially delaminated sample was very cracked and elevated on the perimeter of the cracks. Figure 17-B is a picture of Figure 17-A less magnified and using transmitted light. Cracks and lifted regions of the chromium thin film were noticed in Figure 17-A are seen in Figure 17-B as lighter lines where the light was able to penetrate from the bottom of the sample to the top surface. Figure 17-C shows one of the other thin film samples but this sample is mostly delaminated. The red layer present is unwashed PR applied during spincoating. The dark regions represent the chromium. Figure 17-D shows a further magnified view of the same sample as see in Figure 17-C for higher viewing resolution. When the delamination occurred during spincoating, the remainders of the samples were not spincoated due to fear of the same result. Each of the nine remaining squares was placed in *Cr-Etch* solution to remove the chromium layer and proceed with a new chromium-layer coating. Upon this, the chromium and chalcogenide layer were removed suggesting that the chromium adhered better to the thin film chalcogenide layer than to the glass slide.

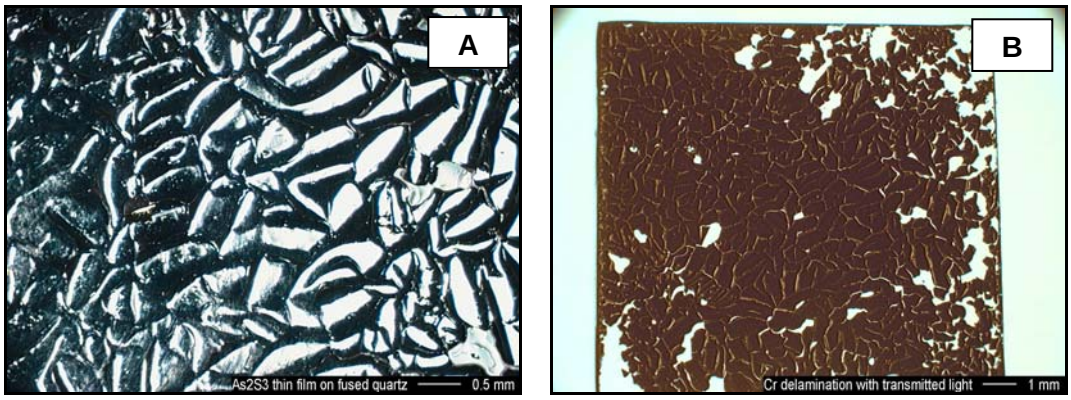

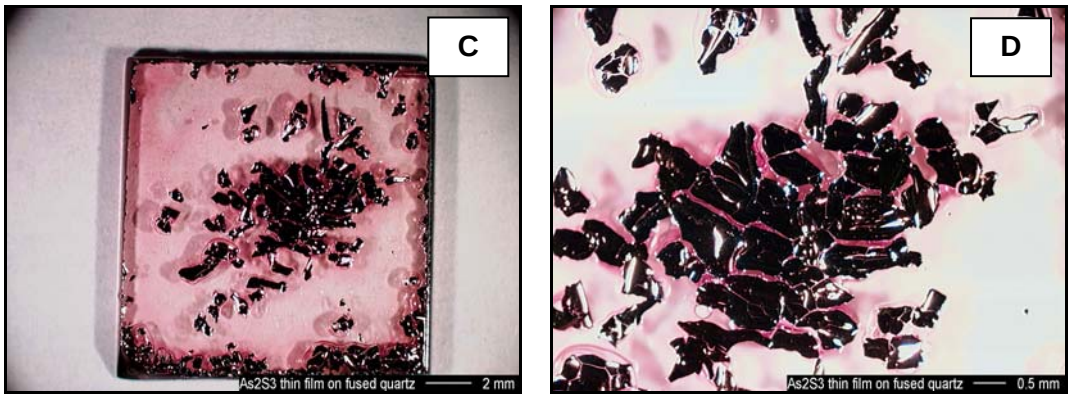

Figure 17-A, -B, -C, and -D. Cr-delamination of As_2S_3 thin films upon spincoating. Figure 17-A shows the chromium surface on an As_2S_3 thin film using reflected light as cracked and elevated on the edges. Figure 17-B shows the same sample as in Figure 17-A but using transmitted light which reveals the cracks around the chromium chunks. Figure 17-C shows a mostly delaminated sample using reflected light and Figure 17-D shows Figure 17-C under a higher magnification.

During the chalcogenide glass etching process more chromium delamination was experienced for the stronger etchants – those with higher NaOH concentration such as 1:1:2, 1:5:10, and 3.4:25:50 with 0.98 M, 0.25 M, and 0.173 M NaOH overall concentration, respectively (see Table 4). When the PR layer was removed from the As_2S_3 sample as seen in Figure 18 using acetone, the chromium layer appeared to have cracked and torn as solid thin layers could sometimes do upon thermal compression. As seen in Figure 18-B, the chromium layer pealing back is quite visible.

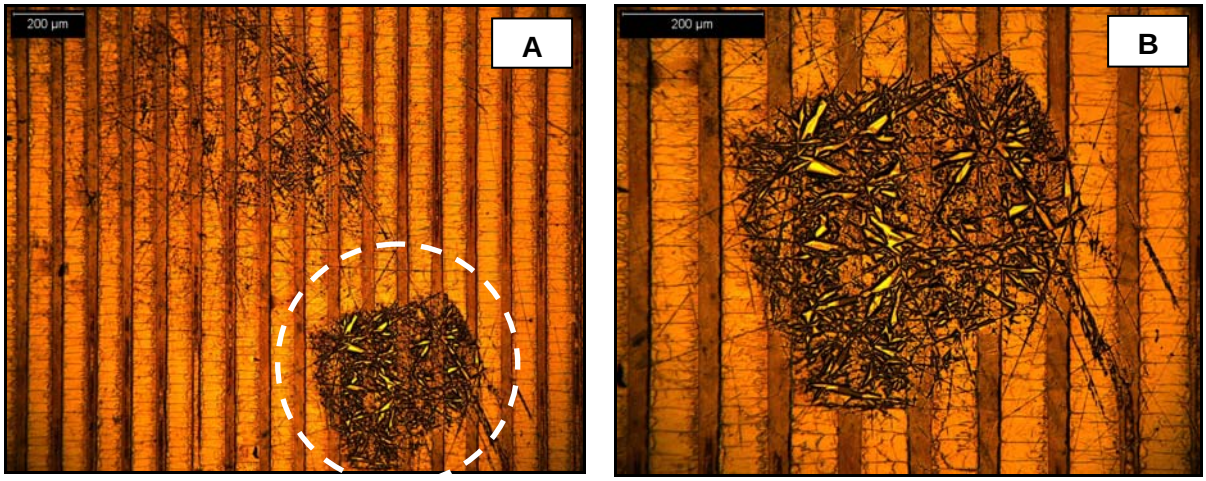

Figure 18-A & -B. Figure 18-A shows chromium delamination from an As_2S_3 sample upon PR-removal that has not yet been subjected to chalcogenide etching. Figure 18-B shows an enlargement of the delamination region in Figure 18-A surrounded by the white dotted line.

During the $As_{24}S_{38}Se_{38}$ glass etching of the sample found in Figure 19, the chromium layer appeared quite fractured. As seen in Figure 19-A, the chromium layer, as denoted by the brighter substance, is cracked and disordered. Figure 19-B shows a different location on the same sample where the chromium layer was undergoing delamination. Some of the chromium step height reference points are seen in Figure 19-B as they lifted off of the glass and folded over (see white circled region). Also, there are regions present

where the delaminated chromium has been washed away by the etchant leaving gaps in the chromium reference as seen by the white arrow in Figure 19-B.

Figure 19-C shows a region of the $As_{24}S_{38}Se_{38}$ sample away from the gratings where the chromium layer is fractured uniformly. The darker regions in Figure 19-C and Figure 19-D show where the chromium was completely delaminated and the glass underneath the chromium is exposed. Figure 19-E and Figure 19-F show more Cr-delamination of reference gratings.

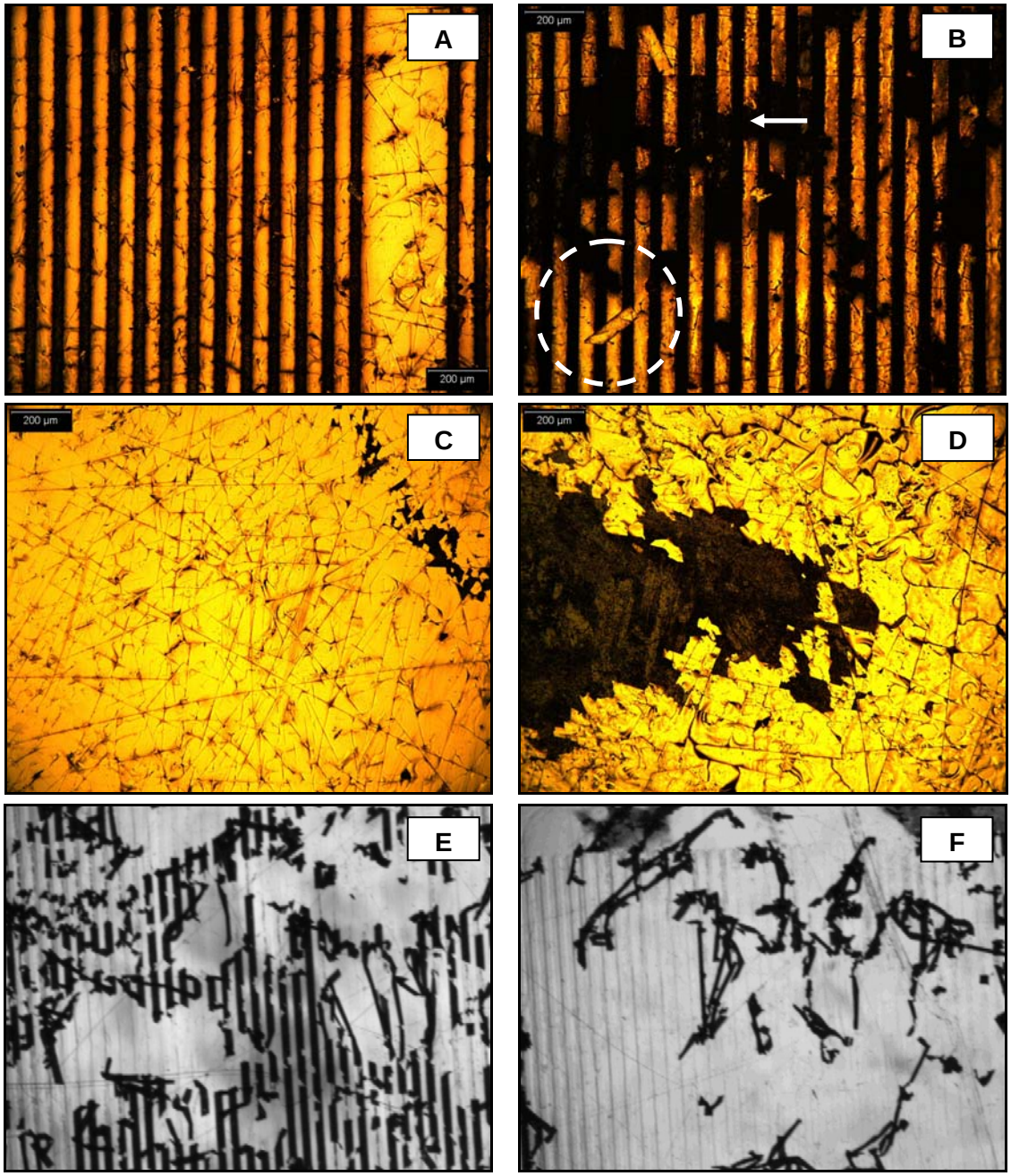

Figure 19-A, -B, -C, -D, -E, and -F. Cr-Delamination of an etched $As_{24}S_{38}Se_{38}$ window from BNW14380-031. Figure 19-A and -B show the grating as elevated locations are covered with chromium which is fractured and delaminating. Figure 19-C and -D show the locations on the sample not covered by gratings undergoing chromium delamination. The dark regions in the pictures are the glass regions and the shining, yellow regions show the presence

of the chromium layer as all pictures were taken using reflected light. Figure 19-E and –F show Cr delamination in the darker regions.

3.4.5 Challenge (5): Inconsistencies in Etching Results

For Challenge (5), the results acquired in the etching studies did vary between samples. As seen in Table 4, the etch rate values obtained for the 1:5:10 etchant using $As_{24}S_{38}Se_{38}$ glass varied quite extensively where rates of 5.777 ± 0.458 nm/s, 15.52 ± 2.56 nm/s, and 2.592 ± 0.510 nm/s were seen for attempts 1, 2, and 3, respectively. Attempts 1 and 3, which differ in etch rate by more than 2-fold (2.23), were performed using windows from the same bulk sample (see Table 4) and attempt 2 was not. Attempts 1 and 2, which differ in etch rate by nearly 3-fold (2.69), were performed using the same etching solution where attempt 3 was performed using a solution prepared, not by starting with the stock solution but by starting with a newly batched 4 M NaOH solution and adding in the IPA and DIW components.

In addition to the differences between the etchants, much variation is noticed in regards to the profilometry data gathered. If using the Si/SiO_2 technology mentioned previously, the step-height and orientation of the ribs left behind after selective etching are extremely uniform and consistent throughout the sample. When looking at Figure 20, a comparison between the Si/SiO_2 system and the chalcogenide glass system, many differences are seen. The sample shown for the Si/SiO_2 system (Figure 20-A, -C, and -E) was etched in BOE (Buffered-Oxide-Etch, an HF/NH_4F mixture), solution for 19 minutes revealing 0.7936 μm step height verified via optical profilometer (Figure 20-E). The sample shown for the chalcogenide glass etching system is the Sample B glass used in measuring the etch rate for the 1:5:10 etchant (Region *ATRC* - see Figure 6) with STEP 7 completed in the etching procedure (see Figure 2). Figure 20-F revealed a step-height of 0.7533 μm via optical profilometer, a similar step-height to Figure 20-E. As seen in the oblique plots, Figure 20-B, the surfaces on the chalcogenide sample are very rough and variable while the top surfaces on Figure 20-A are quite smooth and uniform. The smoother the top reference surface, the more accurate and precise is the measurement taken at that location due to lower variability in the data collected.

When comparing top views Figure 20-D and Figure 20-C, the less-elevated (bluer regions), are less well allocated in Figure 20-D. Figure 20-C shows a very uniform trench depth whereas when measuring the step-height for Figure 20-D, depending on where the measurements were taken, a high degree of variance would be observed. When comparing surface profiles, Figure 20-E displays very sharp, well-defined edges in peak structure whereas Figure 20-F shows not only very poor edges, the depth of the etched trenches is quite difficult to measure. The only accurate way to measure the step-height with the chalcogenide sample is to take an averaged slice through the trench bottoms as was done in Figure 20-F and the result depends solely on where the measurement is taken. Plus, the chalcogenide glass sample seen here is a profilometer measurement taken prior to any chalcogenide glass etching whatsoever as the picture was taken after only chromium etching had been performed. If the sample looks this poor prior to etching the glass, it will look much worse after the etching has taken place; this has been seen on every chalcogenide sample thus far.

In observation of Figure 20-D, upon completion of chromium etching and once the PR is removed to prepare for chalcogenide etching, the valleys of exposed chalcogenide glass should result in a uniform surface. This would be ideal but as seen in Figure 20-B, -D, and -F, the glass top surface is not uniform. This anomaly suggests that the chalcogenide glass is probably somewhat acid-soluble.

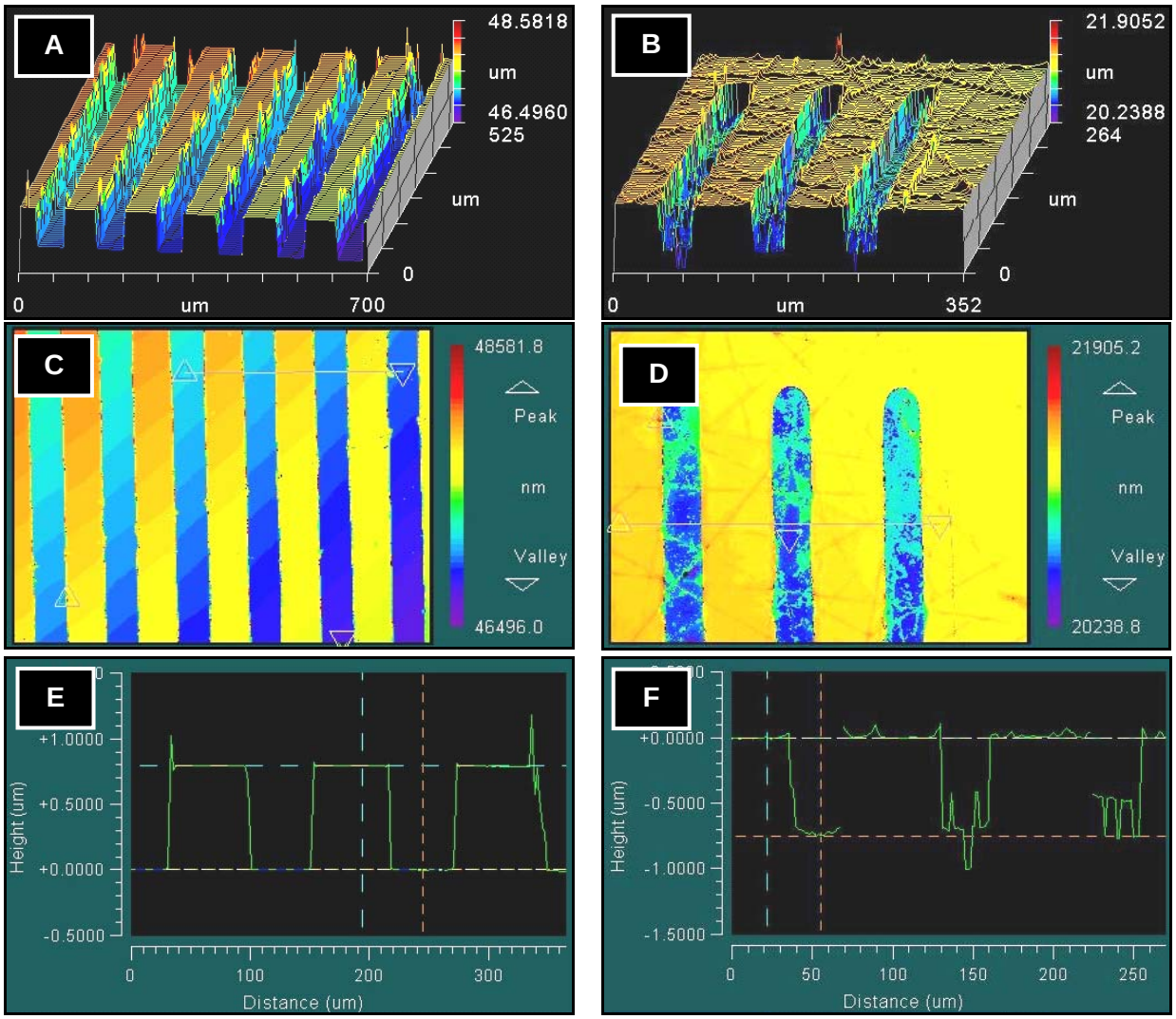

Figure 20-A, -B, -C, -D, -E, and -F. Comparing optical profilometry of Si/SiO_2-etching system (A, C, E) with chalcogenide-etching system (B, D, F). Figure 20-A, -C, and –E show uniform, definite edges for measuring step-heights, whereas Figure 20-B, -D, and –F show extremely variable, rough, and irregular edges making step-height measurements difficult with any high degree of precision or accuracy.

3.4.6 Challenge (6): Variables in Etching Technique

In discussing Challenge (6), eleven different aspects were looked at, which were seen as key variables in the etching technique that should be unchanging in order for the procedure to result in meaningful, accurate, precise, and repeatable results. The eleven different Variable(s) are:

A) Etching solution concentration
B) Solution age
C) Solution volume
D) Sample age
E) Solution temperature
F) Glass sample size
G) Sulfur source in glass sample
H) Chromium-layer thickness

I) Solution agitation
J) Sample cleaning
K) Sample source.

Regarding Variable (A), etching solution concentration, as mentioned in Table 3 and Table 4, the concentration of the etchants used was varied from 0.0134 M NaOH to 0.980 M NaOH, respectively. The relationship of concentration to etching rate observed was not found to be linear for $As_{24}S_{38}Se_{38}$ glasses but it did, however, show a linear trend in the concentration range studied for As_2S_3; see trendlines in Figure 12 and Figure 13 for $As_{24}S_{38}Se_{38}$ and As_2S_3, respectively. As seen in Figure 21, a theorized model of etchant strength over an etching period was generated by comparing Etchant 1 and Etchant 2 the stronger the concentration of the etchant the longer the time that the etchant will show its corresponding etching strength. As most of the OH^- is neutralized, the etchant strength will begin to diminish causing the etch rate to be very different from its starting strength. This variable of concentration gradients among the different etchants can be limited by restricting solution volume, Variable (C).

Variable (B), solution age, was an important aspect of the procedure that was not considered until after the study was completed. As an etchant is used to etch chalcogenide glass, the strength of the etchant is reduced as the solution becomes less basic and less corrosive when the OH^- is neutralized as seen in Equation 9.[4] Equation 9 shows the equilibrium constant, K_c, and how it depends on the concentration of the chalcogenide glass in solution with the etchant, A^+, the concentration of hydroxide ion in solution, OH^-, and the neutral compound created by the joining of the two components to form the complex $A{\cdot}OH$. As the concentration of OH^- in the etchant changes, the etch rate observed while using the etchant will also decrease due to the etching strength showing a positive correlation with the concentration of the etchant. As seen in Figure 21, a plot formed using Equation 10 (a Gaussian Distribution Equation)[vii,5] shows a possible model of the decrease in OH^- concentration over etching time with a particular etchant. Variable (B) needs to be taken into account for further studying.

$$A^+ + OH^- \leftrightarrow A{\cdot}OH, \textbf{ where } K_c = [A{\cdot}OH]_{eq} / [A^+]_{eq}[OH^-]_{eq} \quad \textbf{(10)}$$

$$S_{etching} \approx \int_0^{\infty} \frac{1}{\sigma\sqrt{2\pi}} e^{\frac{-(x-\mu)^2}{2\sigma^2}} dx \quad \textbf{(11)}$$

[vii] A theory for the etch strength, $S_{etching}$, is related to (11 where σ is the standard deviation, x is the x-axis variable where in this case, x is time, and μ is the average.

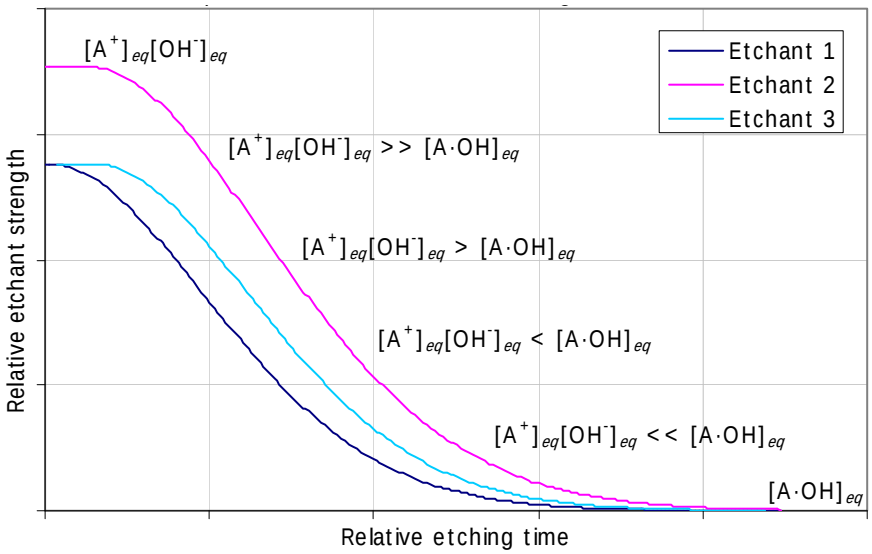

Figure 21. Plot of etchant strength over time of etching as the OH^- is neutralized by the glass components (A^+, here).

Variable (C), solution volume, was also an aspect of the study not enforced during the etching study but needs to be addressed for further etching studies. The volume of solution batched up for the first several etchants was not equivalent. The volume of solution was chosen by a round value of 1:25:50 stock solution (15, 30, 50 mL, etc.) to begin the batching process. Not until midway through the study was a fixed volume of etchant-to-be-batched, V_T^e, implemented (see Equation 2). The greater the volume of etchant, the more etching can take place without as much of a reduction in etching strength as more OH^- is present per total volume. Figure 21 shows three different theoretical etchants, 1, 2, and 3. Etchant 1 and Etchant 3 are shown as they would appear with different volumes of the same etchant concentration. The strengths of each etchant would initially be the same as they would start out with the same overall NaOH concentration although the amount (moles) of OH^- would be greater in the Etchant 3 as it would have greater volume. As the etching proceeded, the NaOH concentration of Etchant 1 would decrease much faster than that of Etchant 2 as the OH^- component (the corrosive factor) was further neutralized. To correct Variable (C), a fixed volume of etchant will be batched for each etchant.

Variable (D), sample age, is a factor when the same sample was used for studying multiple etchants. Instead of preparing an entirely new sample for each etchant, to save time, the same sample was sometimes used to test multiple etchants. In doing so, this left the contour of the sample surface extremely variable and yielded inaccurate results.

Variable (E), solution temperature, is not a large variable in the process. The EMSL cleanroom, where all of the etching was performed, is a highly static environment with ΔT = 2°C (70-72°C) and $\Delta Humidity$ = 4% (30-34%). The temperature and humidity need to be carefully monitored for further studies as this is a key factor in etching rates.

Variable (F), sample size, was not held constant during this study. If the samples are all the same dimensions, they should be affected by and affect the etchant similarly. Due to the different sizes of glass samples already available, different sizes of samples were used.

Variable (G), sulfur source in glass sample, was varied in the $As_{24}S_{38}Se_{38}$ samples. Sample A was manufactured earlier than Sample B. The sulfur source that was used in manufacturing Sample A glass

was from Alfa Aesar and was found to be less pure than advertised (99.999% pure)[6] due to carbon inclusions found upon SEM analysis along with sulfur hydrocarbons and H_2S as verified by FT-IR. Sample B glass was manufactured using Asarco brand sulfur, a much purer form.

Variable (H), chromium-layer thickness, was due to lack of the appropriate Tooling Factor for the FTM on the E-beam in EMSL 1317, yielding a chromium layer deposition variance of 30-1500 nm (see Figure 16). With more time available, this value could be determined very precisely.

Variable (I), solution agitation, was introduced to the sample upon etching via swirling the beaker in hand. This was not a defined variable in the procedure and therefore was not done consistently during each etching. In order to maximize the glass surface exposure to the etchant, sample agitation must be induced via ultrasonicating or stirring with a magnetic stir bar. During etching, ideally the sample surface being etched is placed face-down and suspended on a Teflon platform, so the etched material can be removed via a gravitational migration presenting a fresh sample monolayer for the etchant to react with.

Variable (J), glass sample cleaning, was not perfected during the study. The first method used involved ultrasonicating the samples in acetone for five minutes followed by another five minutes in ethanol. The samples were then placed into the chromium coater. Further methods involved a proceeding plasma clean which, when performing, etched away part of the samples. The plasma cleaning will need to be further explored prior to using in additional etching studies as the process removes carbon inclusions from the sample leaving dimples on the sample surface. A perfectly effective etching method has yet to be established.

Variable (K), sample variation, is a problem due to compositional variation inherent among multiple glass batches. Intrasample variation is not as significant as intersample variation. Samples inclusive from a given glass batch behaved commonly during subjected etching while intersample variation seemed inevitable. See Table 5 for a contrast on the differences between etching results obtained using the same etchant on glass samples from different bulk.

3.4.7 Inconsistencies among Etchants

Figure 22-A shows a consistency in the etch rate data acquired using the windows cut from Sample A bulk glass (see Table 4). The Sample B results acquired were too few of which to establish an accurate trend. Nevertheless, that Sample B results do differ consistently from the results of Sample A glass samples, etching at consistently higher rates as seen from Figure 22-A (also see Table 5). Figure 22-B shows a similarity between the two different etchants used on the Sample A glass samples. The sample run with the new 1:5:10 etchant fit in fairly well with the other data acquired using windows from the same bulk sample (see Table 5). It is important to note the differences between etch rates of different bulk glass samples using the same etchant because if this variation is too great, it might be required to determine etch-rate curves prior to etching any bulk glass that has not yet been studied due to intersample uncertainty. It would be quite unreliable to use the etch rate data acquired for the Sample A glass and Equation 11 to determine the etch time required for a particular depth of etch using the Sample B glass due to the ~3-fold difference between the data.

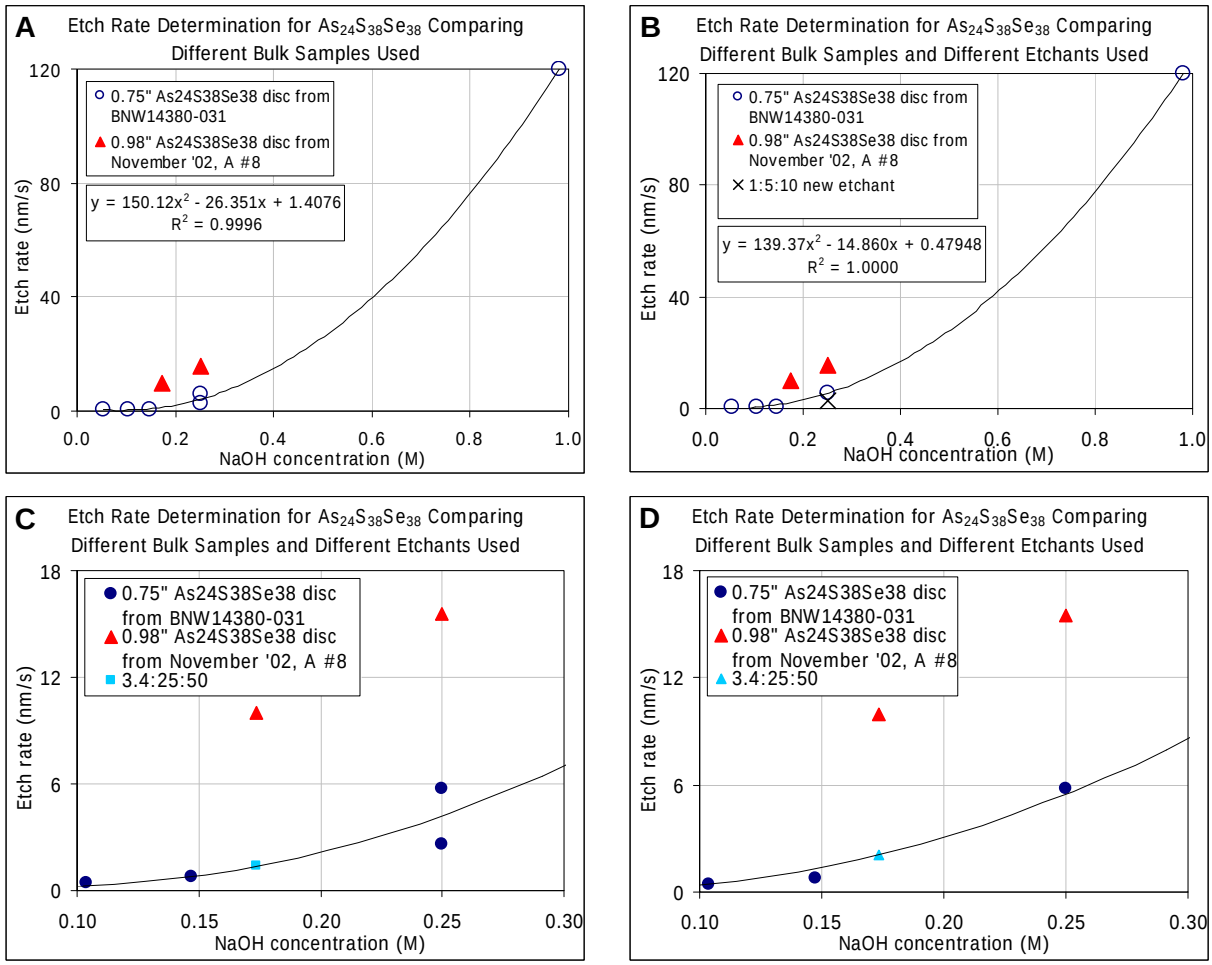

Figure 22-A -B, -C, and -D. In Figure 22-A, all of the Sample A results are grouped whereas in Figure 22-B, all of the Sample A results are grouped except for the results obtained using the new 1:5:10 etchant. Figure 22-C shows a range of Figure 22-A magnified along with an additional calculated point for the presence of a 3.4:25:50 etchant as it would appear on the Sample A trendline presented there. Figure 22-D is similar to Figure 22-C but the range and calculated data observed is from Figure 22-B. Table 5 compares differences between Sample A and B using the different trendlines to calculate an etch rate for Sample A.

Using the trendlines found in Figure 22-A and -B ($y_A = 150.12x^2 - 26.35x + 1.41$ and $y_B = 139.37x^2 - 14.86x + 0.48$, respectively), the calculated etch rate for a theoretical etching using the 3.4:25:50 etchant on Sample A glass was determined and is found in Table 5 as well as it is plotted in Figure 22-C and -D. Table 5 compares the results from Sample A and B showing a consistent *Difference* between the results (8.76 ± 0.933 nm/s) but not a very consistent *Difference Factor* (4.94 ± 2.34 nm/s).

Table 5. Using data acquired for etchants 3.4:25:50 and 1:5:10 to variations in etch rates when using either Sample A or Sample B (see Table 4 and Figure 22-B).[viii]

Sample	*Etchant*	*NaOH(M)*	*Type*	*Rate(nm/s)*	*B - A*	*B/A*
B	3.4:25:50	0.173	Measured	9.988	-	-

[viii] Etch rate data Calculated-C and Calculated-D for 3.4:25:50 etchant on Sample A were determined using the trendlines from Figure 22-A and Figure 22-B, respectively.

A			Calculated-C	1.356	7.9	4.8
A			Calculated-D	2.096	8.6	7.4
B	1:5:10	0.250	Measured	15.52	9.7	2.7
A			Measured	5.777		

When observing the original data obtained for the etchant 1:5:10, the data point was an outlier among the other data points acquired for the $As_{24}S_{38}Se_{38}$ etching. When this outlier was observed, the 1:5:10 etchant was retested using a different, unused, sample of $As_{24}S_{38}Se_{38}$ glass. In doing this, a different etch rate was observed.

As seen in the *Oblique Plots* of Figure 23-A, -B, -C, and -D, it is seen that the surface resolution of the chromium layer is quite variable. Prior to the deposition of the chromium layer in the sample seen in Figure 23, the bulk samples were cleaned in acetone and methanol. The topological variation in the chromium layer is partly due to an unclean surface via surface layer contaminations including the presence of hydrocarbons. In hopes to remedy this anomaly, as mentioned previously, some of the samples were plasma cleaned. Upon doing this, the plasma destroyed the samples by over-etching the surface of the glass. The region which was etched was a semi-uniform pathway inline with the gas intake into the plasma chamber so the etched regions were most likely the regions subjected to the highest temperatures (i.e., the hottest plasma). The second attempt at plasma cleaning was more successful as the time of cleaning was reduced (from 10 minutes with argon followed by 10 minutes with oxygen to 3 minutes with each) as well as the Forward Power (from ~30 W to 10 W). The second plasma cleaning did remove ~200 nm of the test sample in a location with a step-height of 17 µm originally and 16.8 µm afterward in the six total minutes of plasma. Future plasma etching will be reduced to 2 minutes argon followed by 1 minute of oxygen gas at 5 W Forward Power.

3.4.8 Analysis of Data for Determining Etch Rate

In order to determine the etch rate for a particular etchant on a particular sample, data was collected from many different regions (Figure 6) on the glass sample at short time intervals. At each time interval, readings were taken in duplicate or triplicate with the profilometer and screen shots were taken of the data as seen in Figure 23. Each of these data points were assembled into a table as seen in Table 6 where the eight different primary locations on the sample as seen in Figure 6 are relabeled as $Loc_1 - Loc_8$ (where Loc_1 refers to ATLC and the proceeding $Loc_{\#}$ values refer to other regions on Figure 6 proceeding clockwise).

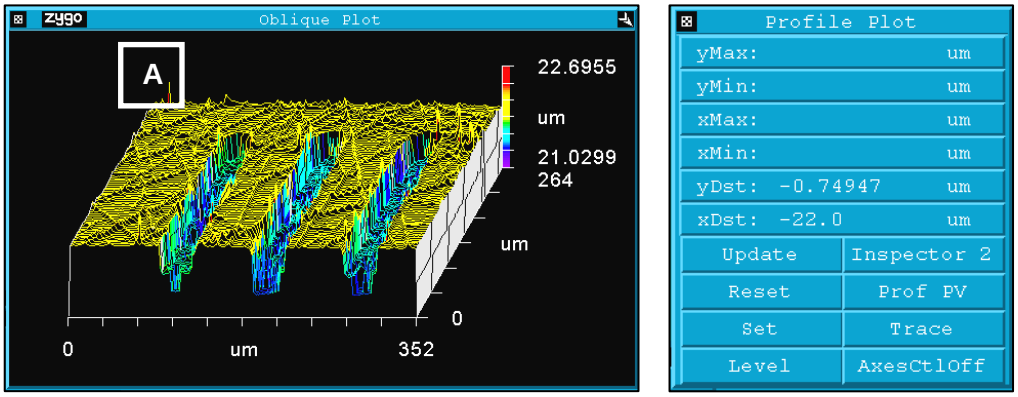

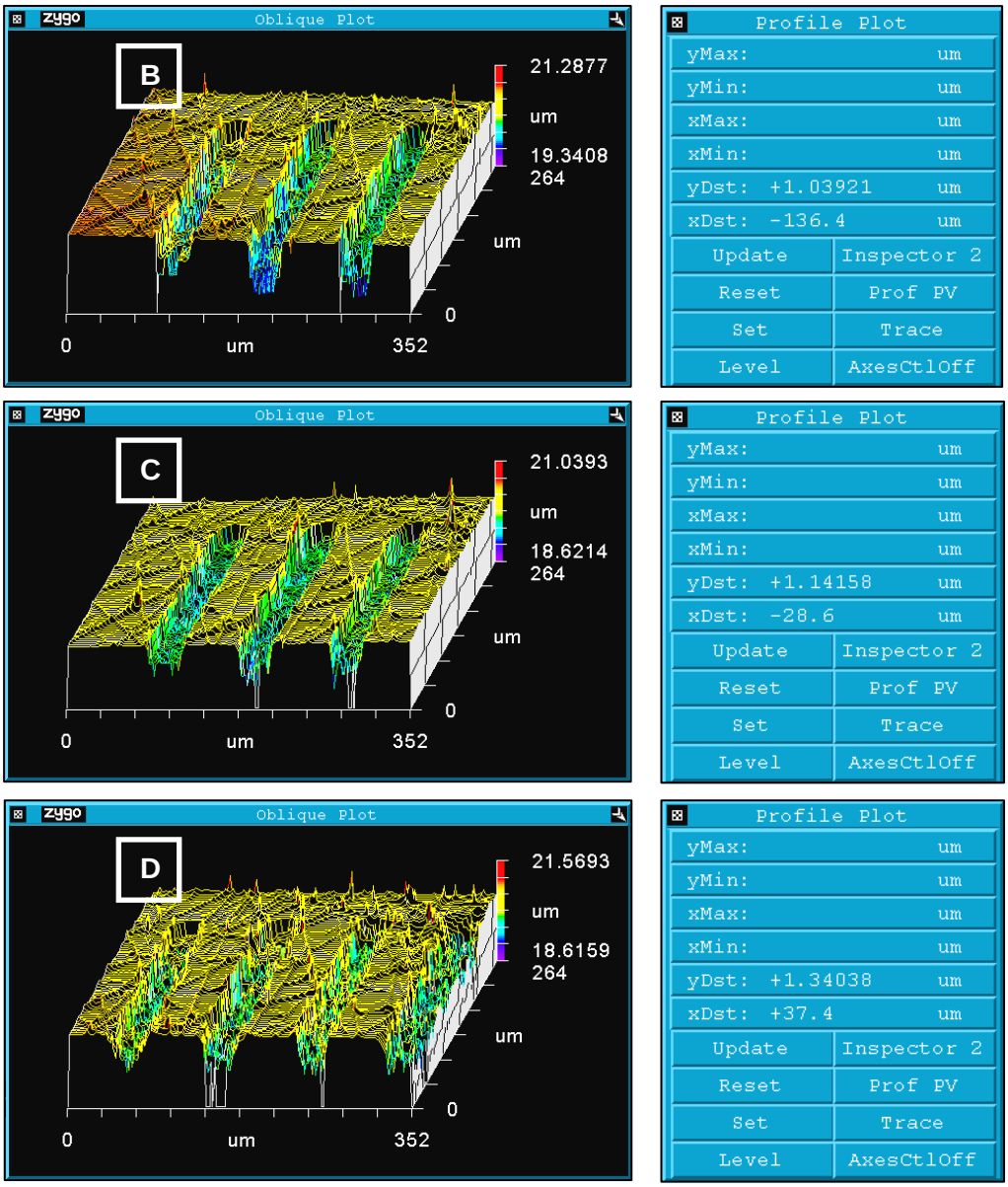

Figure 23-A, -B, -C, and -D. Optical profilometry of Sample B of $As_{24}S_{38}Se_{38}$ during the 1:5:10(2) etching (see Table 4). The Oblique plot is the three dimensional view of the location where the measurement was taken place and the Profile Plot displays the information regarding the step height, or *yDst*, between the Cr peak and the chalco valley. Figure 23-A, -B, -C, and -D are profilometer readings at 0, 14, 24, & 44 seconds, respectively.

Table 6. Step height data, or *yDst* (in nm), collected from various locations ($Loc_{\#}$) around the sample at different time intervals on Sample B for 1:5:10 etchant in determination of etch rate.

Time (sec)	Loc_1	Loc_2	Loc_3	Loc_4	Loc_5	Loc_6	Loc_7	Loc_8
0	749.47	762.16	748.59	491.54	791.87			705.99
14	1039.2	1006.2	1007.7	681.83	1035.3	1009.4		
24	1141.6			784.56		1119.1	547.44	
44	1340.4		1348.2	991.97			800.68	1174.4

Using the data from Table 6, a graphical representation was constructed for comparing the etch rate of the 1:5:10(2) etchant in various locations on the sample that were tested in order to determine the overall etch rate; data from four locations are seen in Figure 10. Equation 12 and Equation 13 were used to determine the change in step-height, $\Delta yDst$, and the change in time, Δt, respectively, using Table 6 data. The *Etch Rate* (*nm/s*) was determined using Equation 14, incorporating data acquired using Table 6, Equation 12, and Equation 13. The values of *Etch Rate* (*nm/s*) are found in Table 7 and can be determined by obtaining the slopes of the linear trendlines Figure 10 which were fit to the data in Table 6.

$$\Delta yDst = yDst_{max} - yDst_{min} \quad \textbf{(12)}$$

$$\Delta t = t_{max} - t_{min} \quad \textbf{(13)}$$

$$Etch\ Rate\ (nm/s) = \Delta yDst * \Delta t * 1000 \quad \textbf{(14)}$$

Table 7. Summary of data acquired using Sample *B* (see Table 4) for 1:5:10 etchant in determination of etch rate.

	Loc_1	Loc_2	Loc_3	Loc_5	Loc_6	Loc_7	Loc_8	Loc_9	Loc_{10}	$\bar{x}$	σ
$\Delta yDst$ (*nm*)	590.9	244.0	599.6	500.4	243.4	109.8	253.2	468.4	376.2	590.9	-
Δt (*s*)	44	14	44	44	14	10	20	44	29.25	44	-
Etch Rate (*nm/s*)	13.43	17.43	13.63	11.37	17.39	10.98	12.66	10.65	13.45	13.43	2.687

In order to determine the concentration of an etchant to batch for a particular rate, the data needed to be modeled. As a spin-off from Figure 13, more trendlines were fit to the Sample A data etched using all of the etchants including the stock solution and those batched by either diluting or concentrating the stock solution (these etchants included: 1:25:50, 2:25:50, 2.94:25:50, 1:5:10(1), 1:5:10(3), and 1:1:2 - see Table 4).

To obtain an etchant operating with a particular etch rate, the trendlines could be used to calculate the overall NaOH concentration needed for the solution as seen in Figure 24. Three trendlines were used in Figure 24, $y_A = 150.12x^2 - 26.35x + 1.41$ (in Figure 24-A from Figure 22-A), $y_B = 139.37x^2 - 14.86x + 0.48$ (in Figure 24-B from Figure 22-B), and $y_C = 942.26x^3 - 200.42x^2 + 14.20x + 0.03$ (in Figure 24-C from Figure 22-C) to fit different sets and regions of the data. Figure 24-A, -B, and -D show how these three 2nd-order trendlines match up on the different regions of the data. Figure 24-C shows a 3rd-order trendline fit to the 1:25:50, 2:25:50, 2.94:25:50, and 1:5:10(1) etchants (see Figure 22-A and -B for explanation of data range used for Figure 24-A and -B). The trendlines in Figure 24-A and -B are quite similar compared to the 3rd-order trendline in Figure 24-C. All of the trendlines fit very nicely to the data points yielding good second and 3rd-order relationships between Etch rate and NaOH concentration using Sample A glass with the stock solution along with concentrated and diluted stock solution etchants.

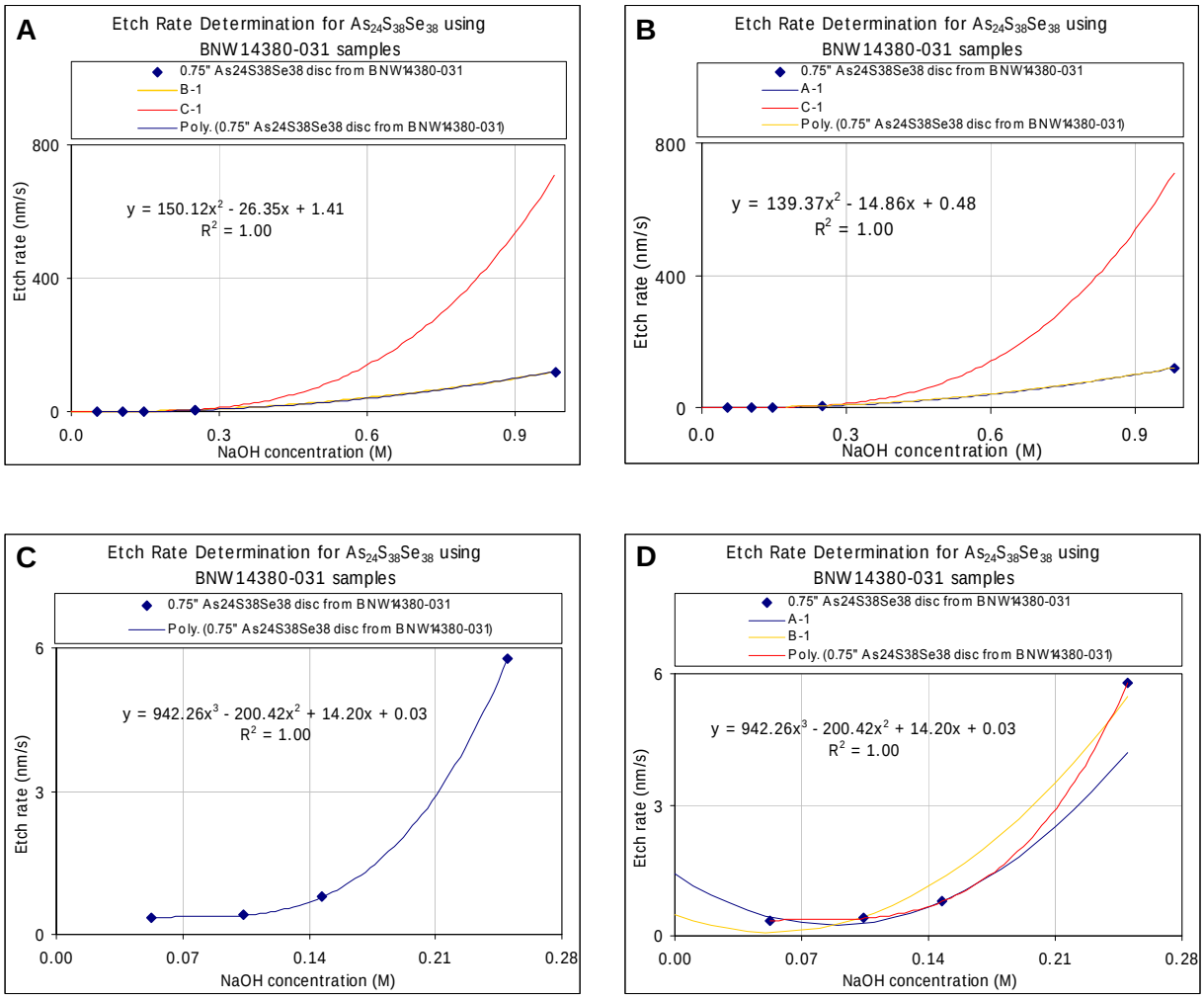

Figure 24-A, -B, -C, and -D. Plots used in determining concentration needed for desired etch rate.

4.0 Conclusions

In determination of the etch rate for these glasses, many challenges were encountered (see the Results and Discussion Section, Challenges and Observations with Etching Techniques). After analyzing all of the results, important differences were observed between etch rate results on glass samples from different bulk glass as revealed in Figure 13, Figure 22, Table 3, and Table 4. In observation of Figure 12 it is seen that the relationship of etch rate of the etchants for chalcogenide glass As_2S_3 and the concentration of NaOH is a linear relationship whereas in Figure 13, the data for $As_{24}S_{38}Se_{38}$, a linear trendline does not fit the composition region. Instead of using linear trendlines for $As_{24}S_{38}Se_{38}$, 2nd and 3rd order equations were implemented as seen in Figure 22 and Figure 24. The trendlines in Figure 12 could be used to calculate the concentration of an etchant required to obtain an etchant expressing a desired etch rate on As_2S_3 glass for a given etch depth in a desired time frame. Similarly, the trendlines in Figure 22 and Figure 24 could similarly be used to do this for $As_{24}S_{38}Se_{38}$ where different equations would be used depending on where in the NaOH concentration range the solution resided.

5.0 Acknowledgements

Pacific Northwest National Laboratory (PNNL) is a multi-program national laboratory operated by Battelle Memorial Institute for the United States Department of Energy under contract DE-AC06-76RLO 1830. Most of the research described in this paper was performed in the Environmental Molecular Sciences Laboratory, a national scientific user facility sponsored by the Department of Energy's Office of Biological and Environmental Research and located at Pacific Northwest National Laboratory. The authors also thank everyone at the Applied Process Engineering Laboratory, especially Evan Jones (managerial support), Teresa Schott (secretarial support), James Martinez (SEM support), and Paul Allen (sample preparation support).

6.0 References

[1] W. Vogel, "Chemistry of Glass," *The American Ceramic Society*, pp. 193-196 (1985).

[2] Kozicki, M.N., Y. Khawaja, A. E. Owen, P. J. S. Ewen, A. Zakery, "As-S/Ag Systems for Integrated Optics," *Sixth International VLSI Multilevel Interconnection Conference, Santa Clara, CA, USA, IEEE Service Center Piscataway NY USA*., (1989).

[3] Love, J. C., K. E. Paul, G. M. Whitesides, "Fabrication of nanometer-scale features by controlled isotropic wet chemical etching," *Adv. Mater.*, **13**(8), pp. 604-607 (2001).

[4] Whitten, K.W., E.D. Raymond, M.L. Peck. *General Chemistry, 6th Edition*. Saunders College Publishing, pp. 715 (2000).

[5] Silbey, R.J., R.A. Alberty. *Physical Chemistry, 3rd Edition*. John Wiley & Sons, Inc (2001). Page 748. This Gaussian distribution equation was adapted from Equation (20.21), 748.

[6] Alfa Aesar Research Chemicals, Metals, and Materials 2003-2004 Catalog. *Sulfur*. Page 1366, Stock No. 10755.